To the Graduate Council:

I am submitting herewith a thesis written by Ngoc-Thuy Dang Nguyen entitled "Performance Analysis of Skip-Glide Trajectories for Hypersonic Waveriders in Planetary Exploration." I have examined the final electronic copy of this thesis for form and content and recommend that it be accepted in partial fulfillment of the requirements for the degree of Master of Science, with a major in Aerospace Engineering.

Gary A. Flandro

_____

Major Professor

We have read this thesis
and recommend its acceptance:

Kenneth R. Kimble

_____

John S. Steinhoff

_____

Acceptance for the Council:

Carolyn R. Hodges

_____

Vice Provost and
Dean of the Graduate School

(Original signatures are on file with official student records.)

Performance Analysis of Skip-Glide Trajectories for Hypersonic Waveriders in Planetary Exploration

A Thesis
Presented for the
Master of Science
Degree
The University of Tennessee, Knoxville

Ngoc-Thuy Dang Nguyen
May 2008

Copyright © 2008 by Ngoc-Thuy Dang Nguyen
All rights reserved.

ACKNOWLEDGEMENTS

I want to take the time to thank all those who believed in me and helped me complete my Master of Science degree in Aerospace Engineering. Without their guidance and support I do not think this would have been possible.

I would like to thank Dr. Flandro for his unconditional support and effort for being there every step of the way in making this possible. I will always be grateful for him taking the time to introduce to me to the topic of hypersonics waverriders and skip and glide trajectories.

I want to thank Dr. Kimble and Dr. Steinhoff as well for supporting me in pursuing this topic and in helping me to complete my degree.

I also want to give out a special thank you to Dr. Daniel, UT Associate Vice President for the University of Tennessee Space Institute (UTSI), for believing in me enough to successfully travel down the long and complicated road in finishing my Master of Science degree at UTSI.

Last but not least, I would like to thank my parents and brother for being there every step of the way during all of this. It was through their unconditional support and encouragement that made all of this possible in the end.

So my heartfelt thanks to all of you.

ABSTRACT

A performance analysis for skip and glide is being studied to investigate the potential usage of waverider technology for interplanetary explorations. While the skip and glide equations themselves were first explored by Eggers, this thesis will implement his equations, but then add waverider technology, to determine the possibility of using trajectory assist to navigate around four planets (Earth, Mars, Jupiter and Venus). All trajectory calculations will be based on the waverider lift-to-drag ratios for various planets to determine the maximum range distance. For this research, skip and glide trajectory will be handled separately to determine which is best suited in covering the most distance for a given planet. Ballistic trajectory will only be mentioned in reference to the derivation of the skip trajectory equation, but will not be covered by itself in this research. Hence, it is possible to study a total of 98 cases of skip trajectories, 12 cases of glide trajectories and any additional cases for the four planets.

Even though the skip and glide equations bear no planetary effect, all results listed in this research are based on Earth with a waverider lift-to-drag (L/D) ratio of 8.61. For a skip trajectory, the maximum number of skips is set to be 3. A high velocity ratio of 1.0 results in a low incidence angle of 0.1˚ with the highest range parameter of 3.52 after 3 skips. A low velocity ratio of 0.2, on the other hand, would result in a high incidence of angle of 39.5˚ with the least range parameter coverage of 0.05.

Applying the same velocity ratio and lift-to-drag to both skip and glide trajectory calculations result in a big percent difference. For example, a L/D = 8.61 and a velocity ratio (V_f) of 1.0 will have a skip range parameter of 3.52 (22,451.09 km) after 3 skips. The glide range parameter, on the other hand, comes out to be 20.60 (131,389.89 km). The percent increase turns out to be around 485.23%. Based on these numbers, it is clear that using a glide trajectory by itself would gain the most range distance for Earth.

TABLE OF CONTENTS

Chapter **Page**

BACKGROUND 1

1.1 INTRODUCTION 1

1.2 SPACE EXPLORATION & MISSIONS TO OTHER PLANETS 2

1.2.1 Mars 3

1.2.2 Venus 3

1.2.3 Jupiter 4

1.3 USING HYPERSONIC VEHICLES FOR INTERPLANETARY SPACE EXPLORATION 5

1.3.1 What are Hypersonic Waveriders? 6

1.4 USING ATMOSPHERIC SKIP & GLIDE TECHNIQUES FOR HYPERSONIC VEHICLES 8

1.5 PREVIOUS RESEARCH 10

1.6 PRESENT RESEARCH 10

1.6.1 Objectives 10

1.6.2 Approach 11

PRELIMINARY CALCULATIONS 13

2.1 METHODOLOGY 13

2.2 ATMOSPHERIC MODELS 14

2.3.1 Earth Atmosphere 14

2.3.2 Mars Atmosphere 17

2.3.3 Atmospheric Models Based on Chapman 18

2.4 SKIP TRAJECTORY 20

2.5 GLIDE TRAJECTORY 21

APPLICATIONS OF WAVERIDERS TO SKIP & GLIDE 22

3.1 PERFORMANCE OF LONG-RANGE HYPERVELOCITY VEHICLES 22

3.2 SKIP TRAJECTORY CALCULATIONS 22

3.3 SKIP TRAJECTORY RESULTS 23

3.4 INCIDENCE ANGLE FOR MAXIMUM RANGE 24

3.5 Glide Trajectory Results 25
3.6 Skip Calculation with Incremental Thrust Addition 26
3.7 Heating Constraints 28
CONCLUSIONS AND RECOMMENDATIONS 29
4.1 Conclusions 29
4.2 Recommendations 30
LIST OF REFERENCES 31
APPENDIX 36
A.1 Skip Trajectory Derivation 37
A.2 Glide Trajectory Derivation 42
A.3 Tables & Figures 45
VITA 72

LIST OF TABLES

Table **Page**

Table A-1: Properties of Mars[17] 45
Table A-2: Properties of Venus[17] 45
Table A-3: Properties of Jupiter[17] 46
Table A-4: Lift-To-Drag Ratios for Various Aircrafts[4, 22, 24] 46
Table A-5: Atmospheric Parameters Various Planets[13] 47
Table A-6: Waverider Lift-To-Drag Ratios[7] 48
Table A-7: Skip Case Studies 49
Table A-8: Maximum Flight Path Angle Results for L/D = 8.61 50
Table A-9: Maximum Range Incidence Angle Results for L/D = 8.61 50
Table A-10: Glide Case Studies for the Four Planets 50
Table A-11: Comparison Between Skip & Glide for Earth at L/D = 8.61 51
Table A-12: Flight Path Angle Results with an Increased of 5% in Velocity Ratio 51
Table A-13: Delta-V For Earth 51
Table A-14: Paramters for Skip Trajectory[14] 51

LIST OF FIGURES

Figure **Page**

Figure A-1: Hubble's Closest View of Mars – August 27, 2003[21] 52
Figure A-2: Planet Venus[17] 52
Figure A-3: Jupiter and Its Moons17 52
Figure A-4: Comparison of Waverider and Generic Hypersonic Configuration[7] 53
Figure A-5: Waverider Model for Earth [7] 53
Figure A-6: Waverider Model for Mars & Jupiter [7] 54
Figure A-7: Waverider Model for Venus 7 54
Figure A-8: Sänger-Bredt *Silbervogel* Aircraft[26] 55
Figure A-9: Parameters of a Periodic Hypersonic Cruise Trajectory 55
Figure A-10: Altitude vs. Density for Earth 56
Figure A-11: Altitude vs. Density for Mars 56
Figure A-12: Altitude vs. ρ/ρo for Earth 57
Figure A-13: Altitude vs. ρ/ρo for Mars 57
Figure A-14: Altitude vs. ρ/ρo for Various Planets 58
Figure A-15: Altitude vs. $\log_{10}(\rho/\rho_o)$ for Various Planets 58
Figure A-16: Velocity Ratio vs. Range Parameter for a Skip Trajectory 59
Figure A-17: Velocity Ratio vs. Range Parameter for a Glide Trajectory 59
Figure A-18: Range Parameter vs. Incidence Angle for n = 1 60
Figure A-19: Range Parameter vs. Incidence Angle for n = 2 60
Figure A-20: Range Parameter vs. Incidence Angle for n = 3 61
Figure A-21: Range Parameter vs. Incidence Angle for L/D = 8.61 & V_f = 0.6 61
Figure A-22: Various Planets Range Parameter vs. Incidence Angle for n = 2 62
Figure A-23: Various Planets Range Parameter vs. Incidence Angle for n = 3 62
Figure A-24: Max. Range Incidence Angle vs. Velocity Ratio for L/D = 8.61 63
Figure A-25: Range Parameter vs. Max. Range Incidence Angle for L/D = 8.61 63
Figure A-26: Range Parameter vs. Velocity Ratio vs. for Various Planets 64
Figure A-27: Earth Range Parameter (Φskip) vs. Incidence Angle (γf) after n = 1 64

Figure A-28: Incidence Angle vs. Lift-To-Drag Ratio with Heating Curve..... 65
Figure A-29: Altitude vs. Temperature for Earth 65
Figure A-30: Altitude vs. Pressure for Earth 66
Figure A-31: Altitude vs. Temperature for Mars..... 66
Figure A-32: Altitude vs. Pressure for Mars..... 67
Figure A-33: Altitude vs. ρ/ρ_o for Venus..... 67
Figure A-34: Altitude vs. ρ/ρ_o for Jupiter 68
Figure A-35: Altitude vs. $\log_{10}(\rho/\rho_o)$ for Earth..... 68
Figure A-36: Altitude vs. $\log_{10}(\rho/\rho_o)$ for Mars 69
Figure A-37: Altitude vs. $\log_{10}(\rho/\rho_o)$ for Venus 69
Figure A-38: Altitude vs. $\log_{10}(\rho/\rho_o)$ for Jupiter..... 70
Figure A-39: Sketch of a Vehicle Executing a 'Skip' Trajectory..... 70
Figure A-40: Sketch of a Vehicle Executing a 'Glide' Trajectory 71

NOMENCLATURE

I. Abbreviations

D	=	drag
g	=	gravitational acceleration
h	=	altitude
L	=	lift
M	=	Mach number
n	=	number of skips during a skip phase
P	=	pressure
PHC	=	periodic hypersonic cruise
r	=	distance from planet center
r_o	=	radius of planet
R	=	range
T	=	temperature
V	=	velocity
V_S	=	velocity of satellite at planet's surface
β	=	constant for exponential atmosphere model
γ	=	angle of flight to horizontal or incidence angle
ρ	=	density
Φ	=	total range

II. Subscripts

Δ	=	change (delta-V)
o	=	sea level
∞	=	free stream
f	=	conditions at end of powered flight
max	=	maximum
s	=	stagnation conditions
total	=	total (range)

CHAPTER I
BACKGROUND

1.1 Introduction

Over the past several decades, the desire to explore other planets in the solar system has become increasingly the main focus in space exploration. The ability to learn and understand the universe, find new resources, determine whether it is possible to colonize other planets, and discover new intelligent life forms have been on the minds on most scientists, researchers and scholars today. While it is part of wanting to advance human life, resources gained from these explorations can translate into physical assets, as well as increase the success rate of human survival in the near future whether it is on Earth itself or any other inhabitable planets.

Until recently, rockets have been used to propel exploration probes and man into space. However, due to their high operational costs, scientists have sought out new means to do explorations. Over the past few decades, new high lift-to-drag ratio hypersonic vehicles, such as a waverider, have been suggested to reduce cost and efficiency. In addition, it was also discovered that it is possible to use the planet's atmosphere to propel or skip the vehicle, like a pebble skipping across the pond, to increase its range of maximum coverage of the entire planet with the least amount of time and fuel consumption. In fact, a waverrider can be thought of as a '*hypersonic glider*' that uses the planet's atmosphere to travel from place to another while requiring no propulsion system whatsoever.

The purpose of this thesis is to combine hypersonic waverider technology with the skip and glide trajectory idea to explore various planets around the solar system. Previous skip and glide studies have only been applied to various supersonic and hypersonic vehicles, but not to waveriders in particular. The ultimate goal is to determine the maximum range distance for a waverider to cover during its mission for any given planet.

Ideally, the vehicle will begin its skip phase once it enters the atmosphere and then eventually '*glides*' out towards the end. This research will determine which type of trajectory, skip or glide, is best suited for a given planet exploration.

1.2 Space Exploration & Missions To Other Planets

As mentioned before, human curiosity and ambition drive mankind to explore the universe around him. "Why should we explore space? Why should money, time and effort be spent researching something with apparently so few benefits? Why should resources be spent on space rather than on conditions and people on Earth?"[23] The answer may lie perhaps in human evolution. According to the European Space Agency, nearly all successful civilizations in human history have been willing to explore. "In exploring, the dangers of surrounding areas may be identified and prepared for. Without knowledge, these dangers have the ability to harm us. With knowledge, their effects or consequences may be lessened."[23]

Space exploration provides mankind with knowledge about the origins of the solar system, planet Earth, and most importantly, about human origins. It helps to answer questions that have intrigued humankind throughout the centuries. The ability to advance human life by collecting data and discovering new resources on other planets can help man adapt as part of his nature and survival. To learn whether life exists or is even feasible on other planets, scientific probes, satellites and space vehicles are sent out to find the answers.

While space may hold many wonders and explanations of how the universe was formed or how it works, it also can be dangerous. Even though the chances of a large asteroid or comet hitting the Earth are small, the ability to colonize other planets will help mankind ensure the continuance of human existence for future generations to come. In the end, the ultimate question remains whether life is possible on any of these other planets in the solar system.

To this very day, Earth is the only planet known to sustain life, but man's ability to adapt could eventually allow him to inhabit other planets and moons. Therefore, in

this thesis, Mars, Venus and Jupiter are chosen to be studied due to their atmospheric properties that can be used for skip and glide applications on hypersonic waveriders.

1.2.1 Mars

Even though Mars, as seen in Figure A-1 (pg. 52), is the fourth planet from the Sun, it is more similar to Earth than any other body in the solar system. Based on past explorations, it was discovered that Mars has mountains and valleys, polar ice caps, and dry riverbeds. Furthermore, it also has seasons, an atmosphere with clouds, winds and dust storms, and a solid rocky surface. When comparing it to all the other known planets besides Earth, Mars also has a moderate climate, which makes it feasible for humans to realistically survive during an exploration venture.[20]

As it is known, Mars's surface consists of many craters and huge volcanoes, but unlike Earth, it lacks the continents that distinctively divides the planet from the vast oceans. The difference between Mars and Earth is that Mars is only half as large as Earth. Its thin atmosphere is comprised of about 95 percent carbon dioxide. The sunlight that reaches Mars is only about half as intense as that on this planet. From past exploration, it has been concluded that the present Mars' atmosphere is too thin and its temperature too cold to allow liquid water to exist. However, past researches have indicated that Mars used to have surface water and groundwater at one point in time. Moreover, Mars also has the largest canyon in the solar system, which would reach from Los Angeles to Chicago if it was located on Earth.[17] Table A-1 (pg. 45) shows some quick facts about Mars.

1.2.2 Venus

One of the most remarkable features about Venus, as seen in Figure A-2 (pg. 52), is that it resembles Earth the most, unlike any other known planets in our solar system. At first glance, if Earth ever had a twin, then it would be Venus. Besides being Earth's nearest planetary neighbor, the two planets are similar in size, mass, density and chemical

composition. In fact, Venus' interior, similarly to Earth's, contains an iron core about 3,000 km in radius and a molten rocky mantle that covers the majority of the planet.[18, 19]

However unlike Earth, Venus has no rainfall, oceans, or strong winds. The atmosphere consists mainly of carbon dioxide, droplets of sulfuric acid, and virtually no water vapor. Also known to be the hottest planet in the solar system, Venus is covered by thick, rapidly spinning clouds that trap surface heat. As a result, this creates a scorched greenhouse-like world with temperatures hot enough to melt metal. Temperatures are usually over 450°C, hotter than the surface of the planet Mercury, which is closest to the Sun. Since these clouds also reflect sunlight, Venus is usually the brightest planet in the sky and is known as the Morning Star and the Evening Star.[18, 19]

Furthermore, exploration satellite images and radar mapping of the planet suggest that Venus' landforms consist of 90 percent volcanoes and lava flows. While more than 1,000 volcanoes or volcanic centers are larger than 20 km in diameter, there may be close to a million volcanic centers that are over 1 km in diameter. In the north region, for example, an elevated region named Ishtar Terra is a lava-filled basin larger than the continental United States.[17, 19] Table A-2 (pg. 45) shows some facts and information about Venus.

In 2005, the European Space Agency announced a plan called '*Venus Express*' to explore the planet in the near future. During its mission, a Soyuz-Fregat rocket from Kazakhstan would fly on a direct trajectory to Venus for 150 days and then study the planet's surface and atmosphere for 450 days. NASA, on the other hand, has no firm plans for a mission to Venus as of today, but it did discuss about sending a robot after 2007 to grab surface samples and return them to Earth for studies.[18]

1.2.3 Jupiter

While Jupiter is the largest planet in the solar system, it is roughly about eleven times the size of Earth's diameter in width. Unlike any rocky planets, Jupiter is a ball of dense hydrogen, helium, water, nitrogen and other gases over a tiny rocky core. Powerful

winds usually dominate the atmosphere with crossing jet streams, lightning and huge hurricane-like storms, such as the one in the Great Red Spot.

According to scientists, the storm has been raging for over 300 years and is about 2 Earth diameters wide.[17] The Great Red Spot can be seen on Jupiter along with four moons: Io (smallest), Europa, Callisto and Ganymede, as seen in Figure A-3 (pg. 52).

Due to its massive size and huge gravity pulls, Jupiter contains 71 percent of the planetary matter in the solar system. As of April, 2003, scientists confirm that Jupiter had about 60 satellites with the possibility of more orbiting its planet.[17] Table A-3 (pg. 46) shows some quick facts about Jupiter.

1.3 Using Hypersonic Vehicles for Interplanetary Space Exploration

In the past, rockets have been used for space traveling, but are no longer necessarily the only means to get into space. Since these rockets had been developed for military missions in the earlier days, they were often considered to be expensive to operate. In addition, a lot of times these rockets experience long delays in determining a possible launch date that would insure that theses missions could be conducted safely.[16]

The idea of using hypersonic vehicles with a high L/D ratio, such as a waverider, is slowly making its way to the space exploration program. In fact, a hypersonic vehicle is an aerospace vehicle, or a hypersonic glider, that can fly at sustained speeds greatly in excess of the local speed of sound.

The term '*hypersonic*' itself was first coined and used by Tsien in 1946 to describe a flow where the flight velocity was much greater than the ambient speed of sound.[2] According to Heiser and Pratt, a hypersonic vehicle of this kind will finally mark the concluding achievements in the world of aviation after work begun by the Wright brothers in 1903.[3] Flight therefore will be possible at virtually any speed and altitude by allowing a vehicle to escape Earth's atmosphere and coast into a nearby permanent orbit for space traveling. With the waverider technology available these days, the next step is

to combine it with the ideal path trajectory to allow its maximum usage of area and range coverage of any given planet.

1.3.1 What are Hypersonic Waveriders?

A waverider is a hypersonic shape that is used to improve the vehicle's hypersonic lift-to-drag ratio. A shock wave is attached to the leading edge where it is contained, thus allowing no spillage of any kind. Through the aid of the contained shock wave, lift is then produced thus allowing the vehicle to gain a significant increase in lift-to-drag ratio. Normally, the vehicle of that particular shape allows the plane to travel at high-speeds of Mach 5 and even higher during ideal hypersonic traveling conditions.[4, 5]

Figure A-4 (pg. 53) shows a comparison model between a waverider and a generic hypersonic configuration. As mentioned previously, the shock wave is attached to the leading edge and then contained, thus not allowing any flow spillage. The generic vehicle, on the other hand, has a detached shock wave at its leading edge. Consequently, it results in flow spillage and a loss in lift.

The waverider concept was first developed by Terence Nonweiler when he designed a re-entry vehicle in 1951.[4, 5, 6] In his initial designs, he considered the waverider as a delta-wing platform with a low wing loading to provide considerable surface area to dump the heat during re-entry. While attempting to create simplified 3 dimensional equations to model his aircraft, he noticed that the shockwave would lead to high pressure under the wing, which could be used for lift. As a result, through this discovery it eventually led to the basic principle of the waverider.

In 1962, Nonweiler published *Delta Wings of Shapes Amenable to Exact Shock-Wave Theory* in the Journal of the Royal Aeronautical Society. In this, he explained that the waverider's wing design must be angled down towards the tips, so the shockwaves can be generated from their leading edges to form a single flat plate shock under the fuselage. The shockwave itself is a lifting surface, thus generating the needed lift with very little physical interaction with the airframe, and thus dramatically lowering heating. Nonweiler's resulting design is a delta-wing with some amount of negative dihedral.

However, one of the disadvantages of using this particular design is that it has more area in contact with the shockwave, therefore causing more pronounced heat dissipation problems.[4, 5, 6]

In 1978, Kuchemann expanded on Nonweiler's idea. He realized that a waverider had a technical possibility by assuming a constant value of the product between propulsive efficiency and aerodynamic efficiency. Using the Breguet range formula, he came to the conclusion that a non-stop trans-atmospheric flight at Mach 8 to the farthest point on Earth is indeed possible.[4]

Over the years, the concept of a hypersonic waverider as an application for foreign planetary atmospheric travels has also been explored, especially in regard to aero-assist for space vehicle trajectory modification. In 1961, Howard London suggested that aerodynamic forces can be used to tailor trajectories and orbits of space by executing an orbital plane change. During his research, he demonstrated that an orbital vehicle, by dipping into the atmosphere of the host planet, could use the aerodynamic lift to obtain the plane change, and the decrement in velocity.[7]

The primary purpose for a waverider design is to create a light-weight disposable lifting surface for interplanetary spacecraft to use while maneuvering over planets with an atmosphere. If used over Venus, for example, the spacecraft could aeromaneuver with the lift provided by the waverider to a degree that no gravitational slingshot could hope to achieve. Moreover, during re-entry, hypersonic vehicles generate lift only from the underside of the fuselage. The underside, which is inclined to the flow at a high angle of attack, creates lift in reaction to the vehicle wedging the airflow downwards. The amount of lift is not particularly high, compared to a traditional wing, but more than enough to maneuver given the amount of distance the vehicle covers.[5] Interests have continued to grow to this very day when the idea of waveriders might possibly replace existing space vehicles, thus giving birth to a potential launch system for a future generation of new spacecrafts.

A sample of a waverider model is shown below in Figure A-5 (pg. 53) based on previous research done on hypersonic waveriders for planetary atmosphere. In this case, the main idea is to show what a potential waverider would look like if it is designed

specifically for Earth at a specific lift-to-drag ratio of 8.61.[7] Figure A-6 and A-7 (pg. 54) show a waverider model for a lift-to-drag ratio of 6.63 for Mars and Jupiter and 11.36 for Venus.

Table A-4 (pg. 46) shows a comparative table for various aircrafts. Starting from the first Wright Flyer with a lift-to-drag ratio of about 8.3 to a typical space shuttle with a lift-to-drag ratio between 1.0 to 4.0, the lift-to-drag ratios are usually not very high. A hypersonic waverider, on the other hand, offers a lift-to-drag ratio range from 8.0 to 15 while a supersonic jet usually has a lift-to-drag ratio of around 8.0. With a high L/D ratio, the waverider would be stable and controllable over a large angle-of-attack range. Selecting a high L/D with a large bank angle would produce a long, turning entry and very high cross range.

New interest in the waverider concept has been sparked after the recent announcement of human exploration to Mars in the near future. Thus, to reduce the cost and to improve the reliability of accessing space, the idea of using a waverider type vehicle might be a possibility for future exploration.[16]

1.4 Using Atmospheric Skip & Glide Techniques for Hypersonic Vehicles

Initial interest of using the waverider as a hypersonic skip and glide aircraft began during the post World War II military era. The idea was to use the vehicle as a '*glider*' to carry a thousand pounds of payload at hypersonic sub-orbital velocity halfway (20,000 km) around the world. During its journey, the waverider would glide and skip along the top of the stratosphere, much like a rock skipping across the surface of the water of a pond.[10]

To avoid heat buildup on the surface and various other parts of the aircraft due to friction with the atmosphere, the waverider would spend much of its flight out of the planet's atmosphere. Any additional heat the craft might pick up while skipping down into the atmosphere may be partially dissipated during the aircraft's re-entry.[9]

This idea was first conceived by Eugen Sänger, a gifted Austrian scientist and engineer, in 1933. In his book *Raketenflugtechnik* (Rocket Flight Technique), he wrote, "In particular that type of rocket flight shall be treated which takes place in the upper layers of the stratosphere with such velocity that the inertial forces due to curvature of the flight path contribute essentially to the lift. This type of rocket flight is the next basic development step beyond the tropospheric flight, accomplished during the last thirty years, and it is the prelude to space flight, the greatest technical problem of our time."[25] While working for the German Air Force, Sänger dreamt of creating the first possibly manned, rocket-powered hypersonic bomber as a glider for extreme flight speed.

In later years, Sänger and his wife Irene Bredt submitted a study entitled, "A Rocket Drive for Long-Range Bombers," which combined for the first time the problems of human integration with those of a rocket-powered glider, operating at the border of space at speeds approaching satellite velocity.[25]

Also known as the '*Silbervogel*' (Silver Bird), this realistic hypersonic design would be used as a dual-use space transporter and global strike aircraft that was sled launched off a monorail. Furthermore to increase the range of the aircraft, Sänger and his wife Irene Bredt proposed that the glider had to skip along the atmosphere rather than using the lift-equal-to-weight glide path.[26] Figure A-8 (pg. 55) shows a design concept of the *Silbervogel*.

This design approach, together with the periodic skip-reentry flight path, was later emulated by the X-20 Dyna-Soar (1957-1963). More recently, studies done by Rudd, Pines and Carter[10, 11] suggest that researchers have found that sub-optimal and optimal periodic cruise trajectories can save fuel consumption from 8 to 45 percent.[10] While periodic hypersonic cruise (PHC) trajectories use a skipping or re-entry trajectory with propulsion impulses to sustain the skipping motion to achieve the desired range, at high speeds, a waverider can skip in and out of the atmosphere due to lightly damped oscillation at a constant angle of attack. This skipping can be continued indefinitely by thrusting at the low point of the trajectory in order to make up for losses due to aerodynamic drag.[10, 11]

1.5 Previous Research

Most past researches based on skip and glide performance analyses have been done by Eggers.[14] In his studies, he derived several equations to determine various types of trajectories used for long-range hypervelocity vehicles.

Eggers wanted to see which type of trajectory, skip or glide, has the most advantage and benefit over the other. In the end, he concluded that during the skip phase, the vehicle will dip into the planetary atmosphere and then make a turn before going right back out of the atmosphere. He also discovered that a lift-to-drag ratio from 1 to 4 will cover the most range distance. However, one disadvantage of using this type of vehicle is that it encounters severe aerodynamic heating.

For a glide phase, on the other hand, the vehicle '*glides*' down into the planet. Based on his work, Eggers[14] realizes that a lift-to-drag ratio greater than 4 is required to cover the maximum range of a planet. The advantage of using this vehicle is that any excess heat generated can be released back into the atmosphere as it goes into the glide phase. It therefore reduces the mass of coolant to be stored to a low quantity.

A more detailed discussion on the skip and glide trajectory performance analysis calculations will be discussed in Chapter 2. There, his equations will be verified by using corresponding plots.

1.6 Present Research

1.6.1 Objectives

The main focus of this thesis is to investigate the potential usage of a skip and glide performance analysis in conjunction with waverider technology for interplanetary exploration. Based on the analyses done by Anderson[7], a waverider can provide high lift-to-drag ratios needed to acquire the desired range distance. These lift-to-drag ratios but have yet to be applied in the skip and glide areas to determine its best application.

Hence, Earth, Mars, Venus and Jupiter are chosen to represent the study in this research, since they contain the required atmospheric conditions necessary to produce a lifting body. The objectives for this research can be summarized as follows:

1. Interplanetary exploration on four planets: Earth, Mars, Venus and Jupiter.

2. Apply lift-to-drag ratios for waveriders to the skip and glide trajectories to determine which is best to acquire the most range distance on those four planets.

3. To determine any optimum values such as lift-to-drag ratio, flight path angle (also known as the incidence angle) and the velocity ratio based on those skip and glide calculations.

1.6.2 Approach

Based on previous calculations derived by Eggers[14], it is possible to study a total of 98 cases of skip trajectories, 12 cases of glide trajectories and any additional cases for the four planets. Beforehand, all equations for skip and glide analyses, which were derived by Eggers[14], will be verified by using corresponding plots and then applied to various planets to determine their best flight ranges. A more detailed outline for the approach is listed below:

1. To determine the feasibility of using high L/D waverider for planetary exploration. Planets chosen for this study are Earth, Mars, Venus and Jupiter. The selection has been based on pervious waverider data available for usage.

2. If the waverider technology is indeed possible, various parameters for optimal flight conditions can be determined the ideal conditions for skip and glide trajectories. For range, which is the main focus of this study, parameters such as

optimum lift-to-drag ratio (L/D), optimum velocity ratio (V_f) and optimum flight path angle (γ_f) are the main focus.

3. For the skip and glide trajectories, the following assumption is made: the path the vehicle will be traveling will not have any curves, cross-path traveling or anything of that nature. Parameters such as lift-to-drag ratio (L/D), velocity ratio (V_f), flight path angle (γ_f), the number of skips involved in the skip phase (n) and the change in velocity (ΔV) if an increased is introduced when adding it to the skip phase are applied and studied.

4. Constraints, such as heating, will also be applied based on existing data from Eggers' past researches[14] to determine the limited flight path angle (γ_f).

5. To calculate the incremental thrust increase during the skip phase. A 5% increase will be applied to a velocity ratio to observe if there is indeed an increase in the range distance.

CHAPTER II
PRELIMINARY CALCULATIONS

2.1 Methodology

The purpose of this section is to verify by Eggers'[14] skip and glide trajectory equations by using generated plots and graphs. Based on his past researches, these types of performance analyses can be calculated using various established equations. In this chapter, a brief summary is offered for each type of trajectory, either skip or glide, and then followed by a short discussion on how the accompanying graphs are generated from the known equations. The idea here is to verify the existing methodology so that later on one can apply those equations to the required case studies for each planet in conjunction with waverider technology.

Figure A-9 (pg. 55) shows an example of what a typical case would be for a skip and glide trajectory once the vehicle enters the planetary atmosphere. Initially, the vehicle will approach the planet at a given velocity ratio (V_f), where it is defined as the ratio of velocity over the satellite velocity. It then dives into atmosphere to undergo its first skip phase at a given flight path angle, manages to turn around and goes right back out at the same flight path angle and velocity ratio. Depending on the number of skips desired, the vehicle will continue to repeat the cycle until it reaches the end and eventually '*glides*' out.

In addition, Figure A-9 also shows a possible case scenario that can be studied for the skip trajectory. A change in velocity (ΔV) is introduced during the skip phase to see if a gain in the velocity ratio can be observed to make a big impact in the overall range distance coverage.

Even though, Figure A-9 shows the case of a vehicle undergoing a skip and glide phase combination, it is not required to do so. In fact, for the purpose of this research, the skip and glide phase will be studied separately to determine which trajectory mode is best suited for a long distance traveling.

2.2 Atmospheric Models

Before any preliminary trajectory calculations can be used to determine the optimal range for a given vehicle, it is necessary to establish a general understanding of the atmospheric model for various planets first. According to Eggers'[14], the skip trajectory calculations are derived based on these models. The equation for skip can be written with the following relationship shown below:

$$\frac{\rho_{\infty}}{\rho_{o}} = e^{-\beta h} \quad (1)$$

Equation 1 gives the ratio between static and total density that is equal to an exponential decay. The total density ρ_0 and constant exponential atmosphere model β, in this case, are assumed to be constant while h is the altitude. In this chapter, Benson's atmospheric models[12] for Earth and Mars are studied in great details and then compared with the results given in Chapman's atmospheric research[13] for various planets. Once Chapman's values for the atmospheric density decay (β) are validated, the atmospheric models for Venus and Jupiter can then be generated. The following atmospheric models for Earth and Mars discussed below are derived based on the NASA Glenn's Beginner's Guide to Aeronautics written by Benson. [12]

2.3.1 Earth Atmosphere

Earth's atmosphere consists of an extremely thin sheet of air extending from the surface of the planet to the edge of space. Within the atmosphere, very complex chemical, thermodynamic, and fluid dynamics effects take place, indicating that the atmosphere is not uniform. Instead, fluid properties are constantly changing with time and place, which it often referred to as the weather.

In this section, the troposphere, lower stratosphere and upper stratosphere are discussed. In the end, an equation is given to determine the density for each layer at varying altitudes.[12]

The Troposphere (h < 11,000 m)

Earth's atmospheric model is defined as three working zones with separate curve fits: the troposphere, lower stratosphere and upper stratosphere. The troposphere runs from the surface of the Earth to 11,000 meters. In the troposphere, the temperature decreases linearly and the pressure decreases exponentially. The rate of temperature decrease is called the lapse rate. According to Benson[12], an accurate representation of the troposphere layer can be given by Equation 2 and 3. For the temperature T (ºC) and the pressure P (kN/m^{-2}) with varying altitude h (m), the following metric units curve fits can be:

$$T = 15.04 - 0.00649 * h \quad (2)$$

$$P = 101.29 * \left[\frac{(T + 273.1)}{288.08}\right]^{(5.256)} \quad (3)$$

where both temperature and pressure are the generic models for the atmosphere at h < 11,000 m.

The Lower Stratosphere (11,000 m < h < 25,000 m)

The lower stratosphere typically runs from 11,000 meters to 25,000 meters. The temperature remains constant in this particular region while the pressure decreases exponentially. The metric units curve fits for the lower stratosphere can be fit to a generic model of:

$$T = -56.46 \quad (4)$$

$$P = 22.65 * e^{(1.73 - 0.000157 * h)} \quad (5)$$

The Upper Stratosphere (h > 25,000 m)

The upper stratosphere model is used for altitudes above 25,000 meters. In this area, the temperature increases slightly while the pressure decreases exponentially. The metric units curve used the upper stratosphere are as follows:

$$T = -131.21 + (0.000299 * h) \quad (6)$$

$$P = 2.488 * \left[\frac{(T + 273.1)}{216.6}\right]^{(-11.388)} \quad (7)$$

Determining Density for Each Zone

The density $\rho\ (kg/cm^3)$ can be derived from the equation of state and is shown as follows for each zone:

$$\rho = \frac{P}{[0.2869 * (T + 273.1)]} \quad (8)$$

As a result, Figure A-10 (pg. 56) shows the relationship for the atmospheric model for Earth's density. Based on Equation 8, the exponential decay curve plotted in Figure A-10 shows that the density increases as the altitude decreases. Furthermore, the upper limit for the density for Earth is around 1.2. A graphical representation for temperature and pressure can be found in the Appendix A.3 (Figures A-29 to A-30, pg. 65-66).

2.3.2 Mars Atmosphere

The Martian atmosphere mainly consists of a thin sheet of gas that primarily consists of carbon dioxide, which extends from the surface of the planet to the edge of the outer space. Similar to Earth's calculations, Mars' atmospheric temperatures and pressures are determined to find the densities.[12]

The Lower Atmosphere (h ≤ 7,000 m)

The lower atmosphere typically runs from the surface of Mars to 7,000 m above. The temperature decreases linearly while the pressure decreases exponentially. The rate of temperature decrease is called the lapse rate. For the temperature T (ºC) and the pressure P (kN/m^{-2}) with varying altitude h (m), the following metric curve fits for the lower atmosphere can be described as follows:

$$T = -31.0 - \left(0.000998 * h\right) \quad (9)$$

$$P = 0.699 * e^{(-0.00009 * h)} \quad (10)$$

The Upper Atmosphere (h > 7,000 m)

The upper stratosphere model is used for any altitudes above 7,000 m. Like in the case of the lower atmosphere, the temperature decreases linearly while the pressure decreases exponentially. The metric curve fits for the upper atmosphere can be determined as follows:

$$T = -23.4 - \left(0.00222 * h\right) \quad (11)$$

$$P = 0.699 * e^{(-0.00009 * h)} \quad (12)$$

Determining Density for Each Zone

Similarly to Earth, the density $\rho\left(\mathrm{kg/cm^3}\right)$ for Mars can be derived from the equation of state for each zone, as shown in Equation 13.

$$\rho = \frac{P}{\left[0.1921 * \left(T + 273.1\right)\right]} \quad (13)$$

However, when comparing the equation of state for the Earth's atmosphere with Mars' atmosphere, the gas constants are notably different. In this case, Mars gas constant is 1,149 while Earth's gas constant is 1,718. This difference is largely due to the fact that the Martian atmosphere is almost entirely made up of carbon dioxide, whiles the Earth's atmosphere consists of a mixture of 78 percent nitrogen and 21 percent oxygen.[12] Furthermore, a graphical representation for the temperature and pressure model can be found in the Appendix A.3 (Figures A-31 to 32, pg. 66-67).

Figure A-11 (pg. 56) shows the relationship for altitude versus density for the atmospheric model for Mars based on Equation 13. Unlike the density graph for Earth (Figure A-10), the exponential decay curve for Mars has an upper limit for density around 0.014.

2.3.3 Atmospheric Models Based on Chapman

To expand the atmospheric calculations to other planets, such as Venus and Jupiter, the atmospheric calculations and graphs derived by Benson[12] in the previous section will be used to compare with the results given by Chapman.[13] Since the main focus is the atmospheric density decay parameter β, Benson's graphs will be compared to Chapman's to determine if the value is close enough to be used for further calculations.

$$\frac{\rho_\infty}{\rho_o} = e^{-\beta h} \quad (1)$$

Using the given equation above and the known values for β given in Table A-5 (pg. 47), a graph for both Earth and Mars can be plotted to compare the resulting curve with the one of Benson's[12].

Figure A-12 (pg. 57) shows altitude versus the density ratio for the case of Earth. When using Chapman's value for Earth's β, the density curve is less than that of approximate curve using Benson's value for β. Nevertheless, it is still a good approximation for the density curve. It can therefore be concluded that any future atmospheric calculations using Chapman's values can be considered within reason without any significant errors.

Figure A-13 (pg. 57) shows the resulting graph of altitude versus the density for Mars. Unlike in the case of Earth, using Chapman's density for Mars results in a higher curve than that of Benson's. However, it is still a good approximation of the density curve.

Figure A-14 (pg. 58) shows the altitude versus density for all the planets. As expected, both Mars and Jupiter share the same density curve since they have the same β. In addition to sharing the same curve, the both also have the highest density curve of all the four planets. The density curve for Venus is the lowest with the lowest listed value for β while Earth ranks in the middle.

Figure A-15 (pg. 58) is another way to represent the same information but in a different format. In this case, the altitude is set against the log of the density, where the resulting curves are linear instead of exponential curves as shown in the previous figure. Like before, Mars and Jupiter share the same density curve that is higher than the other two curves. Venus has the lowest density curve because of its lowest value for β. Several more graphical representations for densities and altitudes of various planets can be found in the Appendix A.3 (Figures A-33 to A-38, pg. 67-70).

2.4 Skip Trajectory

In a skip trajectory, a vehicle enters a given atmosphere of a planet of choice, turns around and then goes back out of the atmosphere. The cycle is repeated again until the desired number of skips has been reached and a certain range distance is acquired. In fact, according to Eggers, he considered the skip trajectory as a '*succession of ballistic trajectories, where each is connected to next by a skipping phase.*'[14]

To derive the skip trajectory equation, Eggers took two main assumptions into consideration:

1. Gravity is neglected. Eggers treated the analysis like a classical impact problem, mainly because of the fact that during the descent in a skip phase, the gravity component is balanced out with the one during the ascent phase.
2. An isothermal atmosphere is assumed, where the temperature does not vary with increasing altitude. Recall that in the previous section where the following equation

$$\frac{\rho_\infty}{\rho_o} = e^{-\beta y} \quad (1)$$

has been introduced to calculate the various atmospheric models. If an isothermal atmosphere is to be considered, then ρ_o and β are assumed to be constant.

Based on those two main assumptions, the skip trajectory equation can be derived as follows where the overall range, Φ_{skip}, is equal to the ratio of the range R over the radius of any given planet, r_o. The resulting equation can then be written as:

$$\Phi_{skip} = \frac{R}{r_o} = \sum_{n=1}^{\infty} \varphi_n = 2\sum_{n=1}^{\infty} \tan^{-1}\left[\frac{\sin\gamma_f \cos\gamma_f}{\frac{1}{V_f^2} e^{\frac{4(n-1)\gamma_f}{L/D}} - \cos^2\gamma_f}\right] \quad (14)$$

where n is number of skips desired, L/D is the lift-to-drag ratio, $V_f = \frac{V}{V_s}$ is the velocity ratio and γ_f is the incidence angle.

Since Eggers assumed this analysis to be analogous to that of an impact problem, the range for each skipping phase is neglected. The total range therefore is simply the sum of the succession of ballistic trajectories.

Using Equation 14, Figure A-16 (pg. 59) shows the velocity ratio versus the range parameter as a function of lift-to-drag ratio. For a given velocity ratio, the range parameter increases with increasing L/D while n starts from 1 and goes up to infinity.

2.5 Glide Trajectory

In addition to the skip trajectories, Eggers[14] also worked out an analysis for the glide trajectories. Before he started to work out on his derivation, he made the following assumptions: any small inclination angle γ to the horizontal can be neglected while constant gravity acceleration is assumed.

Therefore, the maximum range, Φ_{glide}, is equal to the ratio of the range, R, over the radius of the planet, r_o, and can be expressed by the following equation below:

$$\Phi_{glide} = \frac{R}{r_o} = \frac{1}{2}\left(\frac{L}{D}\right)\ln\left(\frac{1}{1 - V_f^2}\right) \quad (15)$$

where L/D is the lift-to-drag ratio and $V_f = \frac{V}{V_s}$ is the velocity ratio.

Figure A-17 (pg. 59) shows velocity ratio versus range parameter as a function of L/D based on Equation 15. Like in the case of the skip trajectory, a range of 0.5 – 6 for the lift-to-drag ratio have been studied to observe the impact on the range. A velocity ratio of 1 is acting as the boundary limit, where the higher the lift-to-drag ratio, the lower the velocity ratio is required to increase the range. A more detailed derivation for the skip and glide trajectory equations can be found in Appendix A.1 and A.2.

CHAPTER III
APPLICATIONS OF WAVERIDERS TO SKIP & GLIDE

3.1 Performance of Long-Range Hypervelocity Vehicles

The main focus of this chapter is to calculate the various skip and glide trajectories for a potential long-range hypervelocity vehicle. Even though, the trajectories of main interest for interplanetary explorations are usually ballistic, skip and glide, ballistic trajectories will not be discussed in this research.

To determine the long-range trajectories, the first step is to use the existing work from Eggers[14] and then use them to determine the different case scenarios for various planets, such as Earth, Mars, Venus and Jupiter. Table A-6 (pg. 48) shows a summary of waverider lift-to-drag ratios for the four planets.

As mentioned in the previous chapter, Eggers'[14] parametric calculation for the skip and glide trajectories can be used to determine the maximum range distance on any planet with existing atmosphere. Since Earth, Mars, Venus and Jupiter were chosen, different parameters, such as lift-to-drag, velocity ratio and the flight path/incidence angle are applied for each planet.

3.2 Skip Trajectory Calculations

In this thesis, however, the flight path angle or incidence angle (γ_f) is varied, while values for velocity ratio (V_f) and lift-to-drag ratio (L/D) remain constant throughout the series of calculations. The variable n, in this case, represents the number of skips in the skip phase. As a result, a total number of 98 cases for skip and 12 cases for glide have been studied for the four planets. Table A-7 (pg. 49) displays a detailed

outline of the various case studies for each planet. The ultimate goal of this calculation is to determine the maximum skip needed for each V_f and L/D.

Note that values for lift-to-drag ratio are based on Table A-6 for waverider for planetary exploration.[7] In this case, an L/D of 6.63 is chosen for Mars and Jupiter. The L/D for Mars will have a corresponding altitude of 20 km. Earth will have an L/D of 8.61 with an altitude of 30 km while Venus will have an L/D of 11.36 with an altitude of 76 km. In addition, the upper and lower limit for the L/D is the proposed range, while the middle value is based on the actual value based on the table.

3.3 Skip Trajectory Results

Figure A-18 (pg. 60) shows the relationship between the range parameter and incidence angle for a single skip. The lift-to-drag ratio (L/D = 8.61) was constant throughout this skip calculation for three the velocity ratios of 0.2, 0.8 and 1.0. The linear curve with a $V_f = 1$ is the boundary limit, and therefore acts as the upper limit for the velocity ratio. In other words, no velocity ratio will be greater than 1. Also note that the type of planet, such as the planet's radius, does not have any bearing in calculating and graphing the results even though the L/D = 8.61 does correspond to the L/D for Earth.

Figures A-19 and A-20 (pg. 60-61) show the same graph relationship between the range parameter versus the incidence angle at n = 2 and n = 3 respectively. A maximum can be observed for the curves with a velocity ratio of 0.80. In fact, for n = 2 with a $V_f = 0.80$, the maximum range is 0.37. For n = 3 and a $V_f = 0.80$, the maximum range is 0.48. A $V_f = 1$ results in a linear curve where it will act as a boundary limit for the velocity ratio, meaning that no velocity ratio will be greater than 1.

Figure A-21 (pg. 61) shows the effect on range of varying the number of skips for a constant L/D and V_f. All three curves share similar patterns where the difference is the peak difference in each curve after a certain number of skips. The higher the number of skips, the larger range parameter will increase to.

Table A-8 (pg. 50) shows the maximum range parameter for 1, 2 and 3 skips at a constant velocity ratio of 0.6. Note that as the number of skips increases, the flight incidence angle gradually decreases while the range distance increases.

Figures A-22 and A-23 (pg. 62) show the range parameter versus velocity ratio for the four planets after 2 and 3 skips respectively. In both cases, the velocity ratio is 1.0 while the L/D varies with the corresponding planets. As it turns out, Venus with the highest L/D of 11.36 has the highest incidence angle of approximately 63˚ after 3 skips. Mars and Jupiter, on the other hand, have a much lower lift-to-drag ratio, L/D = 6.63. With a lower L/D, it therefore requires a lower incidence angle of about 57.5˚.

3.4 Incidence Angle For Maximum Range

The incidence angle corresponding to maximum range was determined for constant L/D as a function of velocity ratio and number of skips.

Figure A-24 (pg. 63) shows the relationship between the maximum range incidence angle and the velocity ratio at a specific lift-to-drag ratio (L/D = 8.61). A larger optimum incidence angle is observed for a lower number of skips. In addition, the lower the velocity ratio is, the higher that maximum range incidence angle will be.

In fact, a $V_f = 0.2$ will have an $\gamma_{max} = 44.5^{\circ}$ after only one single skip with the lowest range distance parameter of 0.02. However, a $V_f = 1.0$ will have the lowest $\gamma_{max} = 0.10^{\circ}$ after one single skip with a range distance parameter of 1.57. (Also note that the slight dip in beginning of each curve is the result of Excel Program trying to fit the best fit curve). A more detailed summary of the results is shown in Table A-9 (pg. 50) for the various cases at an L/D of 8.61.

Figure A-25 (pg. 63) shows the relationship between the range parameter and optimum angle at a specific lift-to-drag ratio (L/D = 8.61). In this particular case, it is observed that the smaller the incidence angle, the greater range distance will be acquired. The higher the angle, the less range is obtained.

3.5 Glide Trajectory Results

In this section, the glide trajectory is evaluated for the various planets. Like in the previous section, all the suggested parameters are based on the Table A-6 data for the waveriders. Three cases were studies for each planet, using the following values for the lift-to-drag ratio shown in Table A-10 (pg. 50).

Figure A-26 (pg. 64) shows the range parameter versus velocity ratio for lift-to-drag ratios corresponding to the waveriders that were optimized for the four planets after 2 and 3 skips respectively if the case scenario of skip and glide combination trajectory is considered. This range then represents the distance that the vehicle would glide after entering the atmosphere from its final skip. The velocity corresponds to the final entry velocity after the final skip.

As expected, the range increases with increasing lift-to-drag ratio for any given velocity. Similarly, a higher entry velocity is required for a lower lift-to-drag ratio to obtain the same range. For the largest lift-to-drag ratio of 11.36 and an entry velocity ratio of 1.0, the '*glide out*' range parameter is approximately 39.24 corresponding to 237,452.65 km for Venus.

Table A-11 (pg. 51) shows a comparison between the results obtained for the skip and glide trajectories. In both instances, they are subjected to the same lift-to-drag and velocity ratio. In addition, for the skip trajectory, the number of skips is set to 3. As it turns out, the range parameter for the glide trajectory is considerably larger than that for the skip after undergoing 3 skips. In fact, with a velocity ratio of 1.0, the range parameter for skip is the highest of 3.52 while glide has a value of 20.60, resulting in almost a 485.23% difference. Even with a low velocity ratio of 0.05, the range parameter for the glide trajectory is still high. The range parameter for the skip trajectory does not even come close to compare, thus ending up with a 180% difference. At this point, based on the data obtained for Earth only, the trajectory covering the most range is the glide trajectory.

3.6 Skip Calculation with Incremental Thrust Addition

In this section, the idea of adding an additional small thrust to the hypersonic waverider to give it an additional boost during the skipping phase. Under normal circumstances, one has to consider the various design criteria on what a fitting rocket model would be the best fit for a specifically designed waverider. Structural and heating considerations are only two examples out of many that need to be considered when adding the additional rocket boost to the waverider.

However, just for the purpose of the next set of calculation, the generalized idea of adding thrust will be applied during the skipping phase. A 5% increase will be added to the velocity ratio for each skipping phase to obtain the new velocity ratio as shown in the equation below:

$$V_{f_{Thrust}} = 1.05 * V_f \quad (16)$$

$$\Delta V_{Thrust} = 1.05 \left(\frac{\Delta V}{V_S} \right) - \left(\frac{\Delta V}{V_S} \right) \quad (17)$$

$$\underline{\Delta V_{Thrust} = 0.05 \left(\frac{\Delta V}{V_S} \right)} \quad (18)$$

A comparison graph is drawn after applying a 5% increase to the velocity ratio after one skip. Starting out with $V_f = 0.6$, the new value for the velocity ratio is $V_f = 0.63$. As shown in Figure A-27 (pg. 64), an increase in the range distance is observed.

As it turns out, with a 5% increase in the velocity ratio during a skip phase, a 13.63% increase in range parameter is observed. Table A-12 (pg. 51) summarizes the results.

To determine if the 5% increase in the velocity ratio is even feasible, the delta-V budget has to be considered. Using the relationship

$$V_f = \frac{V}{V_s} \quad (19)$$

one can the determine the delta-V, ΔV, after a 5% increase in the velocity ratio. Using $V_f = 0.63$ from Table A-12, the following equation can be set up:

$$V_f = \frac{V}{V_S} = 0.63 \quad (20)$$

Applying Equation 18 to 20 above will result in the velocity thrust ratio equation relating to the delta-V.

$$\Delta V_{Thrust} = 0.05 * V_f = 0.05 * 0.63 = \frac{\Delta V}{V_S} \quad (21)$$

where $V_S = 29.783$ km/sec for the average orbital velocity for Earth.

$$\Delta V = 0.05 * 0.63 * V_S = 0.05 * 0.63 * 29.783 \quad (22)$$

The delta-V therefore turns out to be

$$\underline{\Delta V = 0.938 \text{ km/sec for Earth}}$$

Based on Table A-13 (pg. 51), the calculated velocity for Earth is much greater than the given value for the average delta-V per year. It can then therefore be concluded, that this is not feasible just by the fact that the value chosen for the velocity ratio is too large.

3.7 Heating Constraints

Heating constraints comes into play when taking a closer look at the flight path angle. Based on all the case studies for the various planets, some angles are quite high. Unfortunately, a high angle in turn means that more heating will occur on the waverider upon entering the planetary atmosphere.

Using Eggers' work, a cut-off angle can be determined based on the heating constraints. In fact, the following assumptions are taken into considerations:

1. Any gaseous imperfections are to be neglected.
2. Any shockwave boundary layer interaction is to be neglected.
3. The Prandtl number is unity.
4. Any Reynolds analogy can be applied to the analysis.

Table A-14 (pg. 51) shows Eggers' results where he has calculated the maximum incidence angle as function of lift-to-drag ratio based on those heating constraints. Note that an L/D = 0.5 is considered to be a ballistic trajectory and that $V_f = \frac{V}{V_s}$.

Figure A-28 (pg. 65) shows the relationship between the incidence angle and lift-to-drag ratio based on the Table A-14 (pg. 51). Due to the exponential nature of the curve, one can extrapolate a trendline for the heating curve. As it turns out, the higher L/D becomes, the smaller both the incidence angle and velocity ratio will get. In fact, a L/D = 12 will result in an incidence angle of approximately 5º.

In addition, four additional curves are added for the various planets. The maximum incidence angle is plotted against the lift-to-drag for each planet. As expected, since the maximum incidence angle turns out to be so high, all four curves are above the heating curve. In other words, the heating curve acts as a boundary limit. A low L/D = 2, for example will require an incidence angle of about 24º while a high L/D = 12 only needs an angle of 5º.

CHAPTER IV
CONCLUSIONS AND RECOMMENDATIONS

4.1 Conclusions

Based on Eggers' work, a performance analysis is being done to the study of four planets, Earth, Mars, Jupiter and Venus. The idea is to apply the skip and glide trajectory equations to a given planet. To take a step further, waverider technology will be implemented to assist in the space exploration traveling. All calculations therefore will be based on the waverider lift-to-drag ratios for various planets. It is also to be noted that there is no limitation for combining both the skip and glide trajectories to obtain the total range distance covered. However, for the purpose of this research, skip and glide will be handled separately to determine which trajectory is best suited in covering the most distance for any given planet.

Even though the skip and glide equations bear no planetary effect, all results listed in the previous section are based on Earth with a waverider lift-to-drag ratio of 8.61. For a skip trajectory, the maximum number of skips is set to be 3. For example, a high velocity ratio of 1.0 results in a low incidence angle of 0.1˚ with the highest range parameter of 3.52 after 3 skips. A low velocity ratio of 0.2, on the other hand, would result in a high incidence of angle of 39.5˚ with the least range parameter coverage of 0.05.

Applying the same velocity ratio and lift-to-drag to both skip and glide trajectory calculations result in a big percent difference. For example, a L/D = 8.61 and a $V_f = 1.0$ will have a skip range parameter of 3.52 (22,451.09 km) after 3 skips. The glide range parameter on the other hand, comes out to be 20.60 (131,389.89 km). The percent difference turns out to be around 485.23%. It is clear from this that using a glide trajectory by itself would gain the most range distance for any given planet, in this case Earth.

Additional calculations have been made to evaluate the skip trajectory with an incremental thrust increase during the skip phase. A 5% increase has been proposed to the velocity ratio of 0.60 at a L/D = 8.61. A 13.63% increase in the new range distance is observed, coming out to be from 0.22 at a $V_f = 0.60$ to 0.25 at a $V_f = 0.63$. However, when calculating the delta-V (ΔV) the number comes out to be $\Delta V = 938.16$ m/sec. When comparing this value to the average delta-V per year, a large burn is required to acquire more range distance, which is not feasible at this point.

Since all the incidence angles calculated for the skip trajectory are high, heating constraints are applied to determine the boundary limit. Using Eggers' work on heating, a clear distinct line can be drawn where the maximum incidence angle is with its corresponding lift-to-drag ratio. In fact, a low L/D = 2 will require an incidence angle of about 24º while a high L/D = 12 only needs an angle of 5º.

4.2 Recommendations

Now that the preliminary part of the waverider design process is done, the next step would be using the data to determine the required criteria to design the actual waverider vehicle. Using the lift-to-drag ratio, velocity ratio and flight path angle, the shape of the waverider can be determined that undergo the necessary skip-glide trajectory conditions for a specific planet.

In addition, a more detailed look at the rocket boost should be looked into. Structural, heating and any other considerations should be added to determine the best fit for the hypersonic waverider. Also, fuel consumption should also be taking in account as well to see how much fuel is needed and consumed during those projected skip and glide trajectories.

LIST OF REFERENCES

LIST OF REFERENCES

1. Anderson, J. D. Jr., "Compressible Flow – Some History and Introductory Thoughts," Modern *Compressible Flow with Historical Perspective*, 3rd ed., McGraw-Hill, New York, 2002, pp. 2-9.

2. Tsien, H. S., "Similarity Laws of Hypersonic Flows," Journal of Mathematics and Physics, Vol. 25, No. 3, 1946, pp. 247-251.

3. Heiser, W. H., and Pratt, D. T., *Hypersonic Airbreathing Propulsion*, AIAA Education Series, Washington, DC, 1994.

4. Filippone, A., "Hypersonic Waveriders," Advanced Topics in Aerodynamics, Computational Fluid Dynamics, Aeronautics, Propulsion Systems [online], URL: http://aerodyn.org/Wings/waverider.html [cited 26 January 2007].

5. Scott, J., "Hypersonic Waveriders," Aerospaceweb [online], URL: http://www.aerospaceweb.org/design/waverider/main.shtml [cited 25 July 2007].

6. Warwick, G. "Lockheed Martin Falcon hypersonic Attacker," Flight Global [online], URL: http://www.flightglobal.com [cited 25 July 2007].

7. Anderson, J. D., Jr., Lewis, M. J., Kothari, A. J., and Corda, S., "Hypersonic Waveriders for Planetary Atmospheres," AIAA Paper 90-0538, 1990.

8. Andreadis, D., "Scramjets Integrate Air and Space," The Industrial Physics, Vol. 10, No. 4, 2004, pp. 24.

9. Space Transport, “Spacecraft: Hypersoar,” Space Transport [online], URL: http://www.geocities.com/spacetransport/hypersoar.html [cited 25 July 2007].

10. Rudd, L. V., Pines, D. J., and Carter, P. H., “Improved Performance of Sub-Optimal Periodic Hypersonic Flight Trajectories for Long-Range,” AIAA Paper 98-1585, April, 1998.

11. Carter II, P. H., Pines, D. J., and Rudd, L. V., “Approximate Performance of Periodic Hypersonic Cruise Trajectories for Global Reach,” AIAA Paper 98-1644, April 1998.

12. Benson, Tom, “Earth Atmosphere Model,” NASA Glenn Research Center – The Beginner’s Guide to Aeronautics [online], URL: http://www.grc.nasa.gov/WWW/K-12/airplane/atmosmet.html [cited 18 February 2007].

13. Chapman, Dean R., “An Approximate Analytical Method for Studying Entry into Planetary Atmosphere,” NACA TN 4276, May 1958.

14. Eggers, Alfred J., Allen, H. Julian, and Neice, Stanford E., “A Comparative Analysis of the Performance of Long-Range Hypervelocity Vehicles,” NACA TR 1382, 1958.

15. Preston, Carter H., Pines, Darryl J., and Rudd, Lael Eggers., “Approximate Performance of Periodic Hypersonic Cruise Trajectory for Global Reach,” Journal of Spacecraft Vol. 35, No. 6, November-December 1998.

16. Bertin, J. J., and Cummings, R.M., “Fifty Years of Hypersonic: Where We’ve Been, Where We’re Going,” Progress in Aerospace Science, Vol. 39, No. 6-7, August-October 2003, pp. 511-536.

17. Student Science Education Center, “What Do You Know About The Cosmos?” Kid's Cosmos, URL: http://www.kidscosmos.org/kid-stuff.html [cited 07 August 2007].

18. Space.com Staff, “Venus Express Mission Would Explore Sister Planet Mysteries,” Space.com [online], URL: http://www.space.com/scienceastronomy/solarsystem/venus_express_020410.html [cited 07 August 2007].

19. National Aeronautics and Space Administration, “Venus Information,” NASA Jet Propulsion Laboratory [online], URL: http://space.about.com/od/venus/a/venusinfo.htm [cited 07 August 2007].

20. Treiman, A., and Kiefer, W., “Exploring Mars: Educational Brief,” NASA Educational Product EB-1999-02-128-HQ [online], URL: http://www.lpi.usra.edu/expmars/edbrief/edbrief.html [cited 15 February 2007].

21. Crisp, D., and the WFPC2 Science Team, “HubbleSite,” Mars Picture Gallery Database [online], URL: http://hubblesite.org/ [cited 01 March 2007].

22. Wade, Mark, “Russian Rocket Planes?,” Astronautix.com [online], URL: http://www.friends-partners.org/partners/mwade/craftfam/ruslanes.htm [cited 15 August 2007].

23. European Space Agency, “ESA – Space Science – Why Explore Space?,” ESA – Space Science [online], URL:

http://www.esa.int/esaSC/SEMC3VZO4HD_index_0.html [cited 15 August 2007].

24. Scott, J., "Ask Us – Atmosphere & Spacecraft Re-Entry," Aerospaceweb [online], URL: http://www.aerospaceweb.org/question/spacecraft/q0218.shtml [cited 08 October 2007].

25. Ehricke, Krafft A., "Principles of Guided Missile Design," Space Flight, 1960, pp. 26, 38.

26. Hallion, Richard P., "The History of Hypersonics: or 'Back to the Future – Again and Again'," AIAA Paper 2005-0329, January 2005.

APPENDIX

APPENDIX

A.1 Skip Trajectory Derivation

The following derivations of the skip and glide trajectory equations are based on Eggers' work.

Consider Figure A-39 (pg. 70) where a 'skip' trajectory is executed from the atmosphere. A vehicle enters the atmosphere, maneuvers a turn before it goes out from the atmosphere again. That is basic definition for a 'skip' trajectory. Multiple 'skips' can be acquired through the process of repeating the maneuver over and over again until the number of designated skips has been reached.

The end result will be the overall range, or distance traveled during this skip process.

1. Parametric Equations of Motion

To start of the analysis, the parametric equations of motion are applied. Equation (A1) shows that

$$C_L \frac{\rho V^2}{2} A - mg\cos\gamma = \frac{mV^2}{r_e}$$

$$C_D \frac{\rho V^2}{2} A + mg\sin\gamma = m\frac{dV}{dt} \qquad \text{(A1)}$$

are directed perpendicular and parallel to the flight path 's', 'r_e' is the local radius of curvature of the flight path, 'γ' is the local inclination to the horizontal (positive downward), 'ρ' is the local air density, and 'C_L' and 'C_D' are the lift and drag coefficients based on the reference area, 'A', of the vehicle. Note that 'θ' is 'γ' in this case.

2. Classical Impact Problem Idealization

All impact forces are excluded next. Note that during the atmospheric re-entry of ballistic missiles, aerodynamic drag is predominant over the gravity component of $mg\sin\gamma$. In fact, during the descent in a skip phase, the gravity component is balanced out with the one during the ascent.

Gravity then becomes of secondary importance and is therefore neglected. All gravity terms in Equation (A1) are neglected and is therefore reduced down to

$$\frac{1}{2}C_L\rho V^2 A = mV^2\frac{d\gamma}{ds}$$

$$\frac{1}{2}C_D\rho V^2 A = m\frac{dV}{dt}, \quad \text{where } \frac{d\gamma}{ds} = -\frac{1}{r_e}. \tag{A2}$$

3. Isothermal Atmosphere Assumption

Assume an isothermal atmosphere next, where

$$\rho = \rho_o e^{-\beta y} \tag{A3}$$

ρ_o and β are constants, and $y = (r - r_o)$ is the altitude from sea level. Note that $\frac{dy}{ds} = -\sin\gamma$, thus combing Equations (A2) and (A3) will result in

$$\frac{C_L \rho_o A}{2m} e^{-\beta y} dy = \sin\gamma \, d\gamma \qquad (A4)$$

Integrating Equation (A4) will yield

$$\frac{C_L \rho_o A}{2\beta m} e^{-\beta y} = \cos\gamma - \cos\gamma_{en} \qquad (A5)$$

where ρ is taken as zero at the altitude that corresponds to the 'outer reach' of the atmosphere.

Note that Equation (A5) points out an important feature of the skip path: $\cos\gamma$ is a single-valued function of altitude. Since γ proceeds from positive to negative values, it is therefore evident that

$$\gamma_{en_{n-1}} = -\gamma_{ex_n} \qquad (A6)$$

where the subscripts 'en' and 'ex' are designated to the atmospherics entrance and exit conditions, the numbers 'n – 1' and 'n' refer to the number of successive skips.

Since

$$\frac{dV}{dt} = V\frac{dV}{ds} = \frac{1}{2}\frac{dV^2}{ds}$$

Equation (A2) may be combined to obtain the following

$$\frac{1}{2}\frac{dV^2}{ds} = \frac{V^2}{L/D}\frac{d\gamma}{ds} \qquad (A7)$$

At constant L/D, integrate to get

$$\frac{V_{ex_n}}{V_{en_{n-1}}} = e^{\frac{\gamma_{ex_n} - \gamma_{en_{n-1}}}{L/D}} \qquad (A8)$$

Apply Equation (A6) to (A8), and the following expression can be written as

$$\frac{V_{ex_n}}{V_{en_{n-1}}} = e^{-\frac{2\gamma_{en_{n-1}}}{L/D}} \qquad (A10)$$

Equation (A10) shows the velocity relationship between the beginning and end of a skip to the lift-to-drag ratio (L/D) and the entrance angle (γ) of the vehicle to the atmosphere.

In addition, from Equation (A6), it also can be established that the entrance angle for each skip in the trajectory is the same.

$$\gamma_{ex_n} = \gamma_{en_{n-1}} = \ldots = \gamma_f$$

Apply that to Equation (A10)

$$\frac{V_{ex_n}}{V_{en_{n-1}}} = e^{-\frac{2\gamma_f}{L/D}} \quad (A11)$$

Since Eggers' defined that a skip trajectory ought to be thought of as a 'succession of ballistic trajectories, each connected to the next by a skipping phase', the ballistic equation is now applied to obtain the total flight range of the vehicle.

$$\Phi_{ballistic} = \frac{R}{r_o} = 2\tan^{-1}\left(\frac{\sin\gamma_f \cos\gamma_f}{\frac{1}{V_f^2} - \cos^2\gamma_f}\right) \quad (A12)$$

From Equation (A12), the range of the nth ballistic segment of the trajectory can be rewritten as

$$\varphi_n = 2\tan^{-1}\left(\frac{\sin\gamma_f \cos\gamma_f}{\left(\frac{V_s}{V_{ex_n}^2}\right)^2 - \cos^2\gamma_f}\right) \quad (A13)$$

To be consistent with the idealization of the skipping process and treating it like a classical impact problem, neglect the contribution to range of each skipping phase so that the total range is simply the sum of the ballistic contributions.

From Equations (A12) and (A13), the total range for a skip trajectory can finally be written as

$$\Phi_{skip} = \frac{R}{r_o} = \sum_{n=1}^{\infty} \varphi_n = 2\sum_{n=1}^{\infty} \tan^{-1}\left(\frac{\sin\gamma_f \cos\gamma_f}{\frac{1}{V_f^2} e^{\frac{4(n-1)\gamma_f}{L/D}} - \cos^2\gamma_f}\right) \quad (A14)$$

where at any given velocity at the end of a flight, there exists a definite skipping angle which maximizes the range of vehicle at a certain lift-to-drag ratio.

A.2 Glide Trajectory Derivation

1. Parametric Equations of Motion

Figure A-40 (pg. 71) shows a sketch of a vehicle undergoing a 'glide' maneuver. Note that 'θ' is 'γ' in this case. Like in the skip trajectory analysis, the parametric equations of motion are used. Equation (B1) show that

$$L - mg\cos\gamma = -\frac{mV^2}{r_e}$$

$$-D + mg\sin\gamma = m\frac{dV}{dt} \qquad \text{(B1)}$$

are normal and parallel to the direction of flight.

2. Small Inclination Angle Assumption

Assume a small inclination angle γ to the horizontal, where $\cos\gamma \approx 1$, $\sin\gamma \approx \gamma$ with constant gravity acceleration (i.e. $\frac{r}{r_o} \approx 1$). The following relationships can be derived.

$$\frac{dV}{dt} = V\frac{dV}{ds} = \frac{1}{2}\frac{dV^2}{ds} \qquad \text{(B2)}$$

$$-\frac{1}{r_e} = \frac{d(\psi - \gamma)}{ds}$$

$$-\frac{d\psi}{ds} = \frac{\cos\gamma}{r} \approx \frac{1}{r_o}$$

where ψ is the remaining range (ψ = total range (Φ) - partial range (φ)). Equation (B1) can then be rewritten in the forms

$$L = -mV^2 + mg - \frac{mV^2}{r_o}$$

$$D = -\frac{1}{2} m \frac{dV^2}{ds} + mg\gamma \qquad \text{(B3)}$$

Dividing the first Equation (B3) by the second will result in the following differential equation

$$g\left(1 - \frac{L}{D}\gamma\right) + \left(\frac{1}{2}\frac{L}{D}\frac{dV^2}{ds} - V^2\frac{d\gamma}{ds}\right) - \frac{V^2}{r_o} = 0 \qquad \text{(B4)}$$

The terms L/D $g\gamma$ and $V^2\frac{d\gamma}{ds}$ are neglected based on Eggers' work in Appendix A, so that Equation (B4) reduces to

$$\frac{dV^2}{ds} - \frac{2}{r_o\left(L/D\right)}V^2 + \frac{2g}{L/D} = 0 \qquad \text{(B5)}$$

Since $V_s^2 = gr_o$, Equation (B5) can be integrated for constant L/D to give the velocity in nondimensional form

$$V^2 = 1 - (1 - V_f^2)\, e^{\frac{2\varphi}{L/D}} \qquad \text{(B6)}$$

Equation (B6) allows the velocity to become a function in term of range. In fact, Eggers notes with a reference to Sanger that this particular expression is can be termed as the equilibrium trajectory, where the gravity force is balanced by the aerodynamic lift and centrifugal force. Equation (B7) demonstrates it while Equation (B8) is expressed in terms of velocity.

$$\frac{L}{W} \approx 1 - V^2 \qquad \text{(B7)}$$

where 'L' is the lift and 'W' is the weight.

$$V^2 = \frac{1}{1 + \dfrac{C_L A V_s^2 \rho}{2mg}} \qquad \text{(B8)}$$

Now it is intuitively obvious that as the maximum range is approached, $L/W \to 1$ and V^2 becomes small compared to one (see Equation (B7)).

Therefore, the maximum range for the glide trajectory can be written as

$$\Phi_{glide} = \frac{R}{r_o} = \frac{1}{2}\left(\frac{L}{D}\right) \ln\left(\frac{1}{1 - V_f^2}\right) \qquad \text{(B9)}$$

A.3 Tables & Figures

Table A-1: Properties of Mars[17]

Topic	Data
Diameter	6794.4 km
Density	3.94 g/cm^3
Mass	6.421 x 10^{23} kg
Volume	1.643 x 10^{11} km^3
Temperature Range	-140° C to 20° C
Atmosphere	Mostly Carbon Dioxide
Winds	Up to 100 km/hr
Moons	2
Average Distance from Sun	227,940,000 km
Orbital Period	1 Years, 320 Days, 18.2 Hours
Rotation	1 Days, 0.67 Hours
Tilt	25.19°
Rings	No
Composition	Iron Oxides and Silicates
Magnetic Field	Slight

Table A-2: Properties of Venus[17]

Topic	Data
Diameter	12,104 km
Density	5.25 g/cm^3
Mass	4.869 x 10^{24} kg
Volume	9.284 x 10^{11} km^3
Temperature Range	-45° C to 464° C
Atmosphere	97% Carbon Dioxide, Nitrogen
Winds	350 km/hr
Moons	None
Average Distance from Sun	108,200,000 km
Orbital Period	0 Years, 224 Days, 16.8 Hours
Rotation (Retrograde)	243 Days, 0.5 Hours
Tilt	177.36°
Rings	None
Composition	Iron Core, Silicate Surface
Magnetic Field	Slight

Table A-3: Properties of Jupiter[17]

Topic	Data
Diameter	142,984 km
Density	1.33 g/cm^3
Mass	1.900 x 10^{27} kg
Volume	1.377 x 10^{15} km^3
Temperature Range	-163° C to > -121° C
Atmosphere	Hydrogen, Helium, Methane
Winds	Up to 150 m/s
Moons	60
Average Distance from Sun	778,330,000 km
Orbital Period	11 Years, 315 Days, 1.1 Hours
Rotation	0 Days, 9.925 Hours
Tilt	3.13°
Rings	Yes
Composition	Hydrogen and Helium
Magnetic Field	Extends 1,600,000 km

Table A-4: Lift-To-Drag Ratios for Various Aircrafts[4, 22, 24]

Type of Aircrafts	L / D
Wright Flyer I (1903) (Subsonic)	8.3
Supersonic Jet Transport (Concorde)	8.0
Semiballistic Apollo Type Spacecraft	0.5
Space Shuttle	1.0 – 4.0
Potential Waverider Model	8-15

Table A-5: Atmospheric Parameters Various Planets[13]

Planet	r (km)	Gases	β^{-1} (m)
Earth	6,378.15	N_2, O_2	7,162.8
Venus	6,051.90	CO_2, N_2	6,096
Mars	3,402.5	N_2, CO_2	18,288
Jupiter	71,402	H_2, CH_4	18,288

Table A-6: Waverider Lift-To-Drag Ratios[7]

Planet	M	Altitude (km)	L/D
Earth	19	30	8.61
Venus	19	30	9.14
Venus	30	30	14.46
Venus	30	76	11.36
Mars	19	20	6.63
Mars	19	30	5.38

Table A-7: Skip Case Studies

L/D	n	V_f		L/D	n	V_f	
5	1	0.20		8.61	1	0.60	
5	2	0.20		8.61	2	0.60	Earth
5	3	0.20		8.61	3	0.60	
5	1	0.50		8.61	1	1.00	
5	2	0.50		8.61	2	1.00	Earth
5	3	0.50		8.61	3	1.00	
5	1	0.60		10	1	0.10	
5	2	0.60		10	2	0.10	
5	3	0.60		10	3	0.10	
5	1	0.80		10	1	0.20	
5	2	0.80		10	2	0.20	
5	3	0.80		10	3	0.20	
5	1	0.99		10	1	0.50	
5	2	0.99		10	2	0.50	
5	3	0.99		10	3	0.50	
5	1	1.00		10	1	0.60	
5	2	1.00		10	2	0.60	
5	3	1.00		10	3	0.60	
6.63	1	0.10		10	1	0.80	
6.63	2	0.10	Mars /	10	2	0.80	
6.63	3	0.10	Jupiter	10	3	0.80	
6.63	1	0.20		10	1	0.99	
6.63	2	0.20	Mars /	10	2	0.99	
6.63	3	0.20	Jupiter	10	3	0.99	
6.63	1	0.50		11.36	1	0.10	
6.63	2	0.50	Mars /	11.36	2	0.10	Venus
6.63	3	0.50	Jupiter	11.36	3	0.10	
6.63	1	0.80		11.36	1	0.50	
6.63	2	0.80	Mars /	11.36	2	0.50	Venus
6.63	3	0.80	Jupiter	11.36	3	0.50	
6.63	1	0.99		11.36	1	0.99	
6.63	2	0.99	Mars /	11.36	2	0.99	Venus
6.63	3	0.99	Jupiter	11.36	3	0.99	
8	1	0.50		15	1	0.10	
8	2	0.50		15	2	0.10	
8	3	0.50		15	3	0.10	
8	1	0.99		15	1	0.50	
8	2	0.99		15	2	0.50	
8	3	0.99		15	3	0.50	
8.61	1	0.20		15		0.99	
8.61	2	0.20	Earth	15	2	0.99	
8.61	3	0.20		15	3	0.99	

Table A-8: Maximum Flight Path Angle Results for L/D = 8.61

n	V_f	γ_f (degrees)	$\Phi_{skip, max}$
1	0.6	38.5	0.22
2	0.6	36.5	0.37
3	0.6	34.5	0.48

Table A-9: Maximum Range Incidence Angle Results for L/D = 8.61

n	V_f	γ_{max} (degrees)	$\Phi_{skip, max}$
1	1.0	0.1	1.57
2	1.0	0.1	2.70
3	1.0	0.1	3.52
1	0.6	38.5	0.22
2	0.6	36.5	0.37
3	0.6	34.5	0.48
1	0.2	44.5	0.02
2	0.2	41.5	0.03
3	0.2	39.5	0.05

Table A-10: Glide Case Studies for the Four Planets

Earth Case	L/D	Mars Case	L/D	Venus Case	L/D	Jupiter Case	L/D
EG1	5	MG1	5	VG1	8	JG1	5
EG2	8.61	MG2	6.63	VG2	11.36	JG2	6.63
EG3	10	MG3	10	VG3	15	JG3	10

Table A-11: Comparison Between Skip & Glide for Earth at L/D = 8.61

n	V_f	$\Phi_{skip, max}$	$\Phi_{skip, max}$ (km)	$\Phi_{glide, max}$	$\Phi_{glide, max}$ (km)	Absolute Percent Difference (%)
3	1.0	3.52	22,451.09	20.60	131,389.89	485.23
3	0.6	0.48	3,074.27	1.48	9,439.66	207.05
3	0.2	0.05	318.91	0.14	892.94	180

Table A-12: Flight Path Angle Results with an Increased of 5% in Velocity Ratio

n	L/D	V_f	γ_f (degrees)	Φ_{skip}
1	8.61	0.60	38.5	0.22
1	8.61	0.63	37.5	0.25

Table A-13: Delta-V For Earth

Maneuver	Average delta-V per year (m/sec)	ΔV (m/sec)
Drag Compensation in 400-500km LEO	< 25	938.16
Drag Compensation in 500-600km LEO	< 5	938.16

Table A-14: Paramters for Skip Trajectory[14]

L/D	γ_f (degrees)	V_f
6	12.5	0.275
4	17.0	0.315
2	24.0	0.525
1	27.5	0.620
0.5	30.0	0.650



Figure A-1: Hubble's Closest View of Mars – August 27, 2003[21]

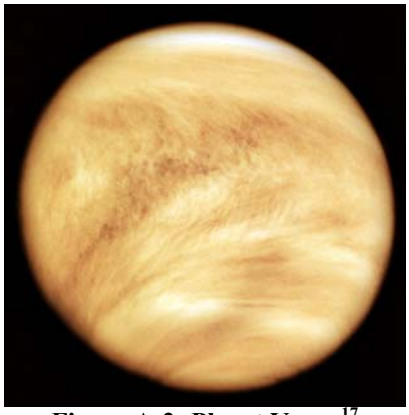

Figure A-2: Planet Venus[17]



Figure A-3: Jupiter and Its Moons17

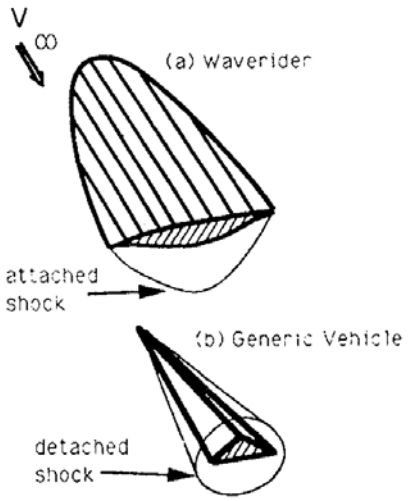

Figure A-4: Comparison of Waverider and Generic Hypersonic Configuration[7]

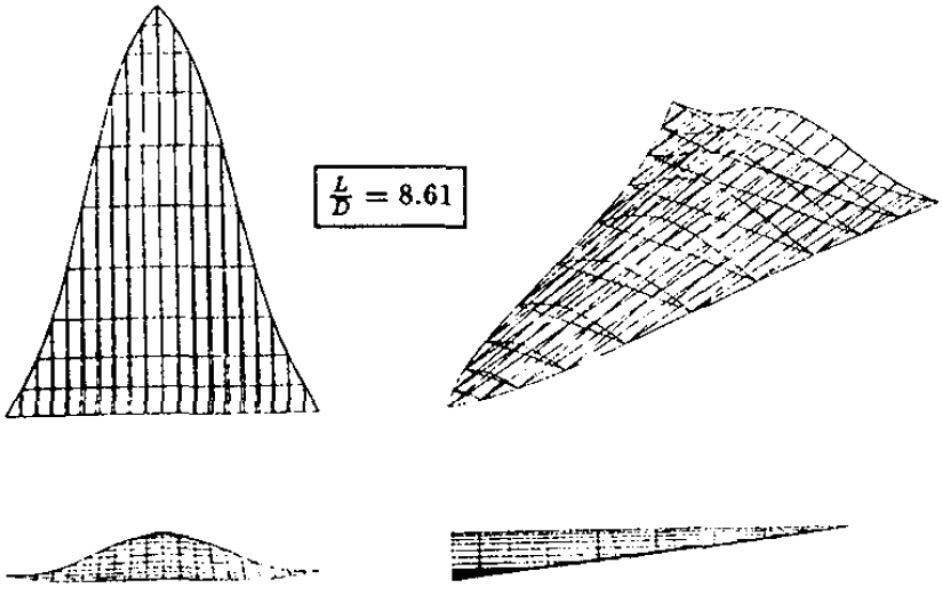

Figure A-5: Waverider Model for Earth [7]

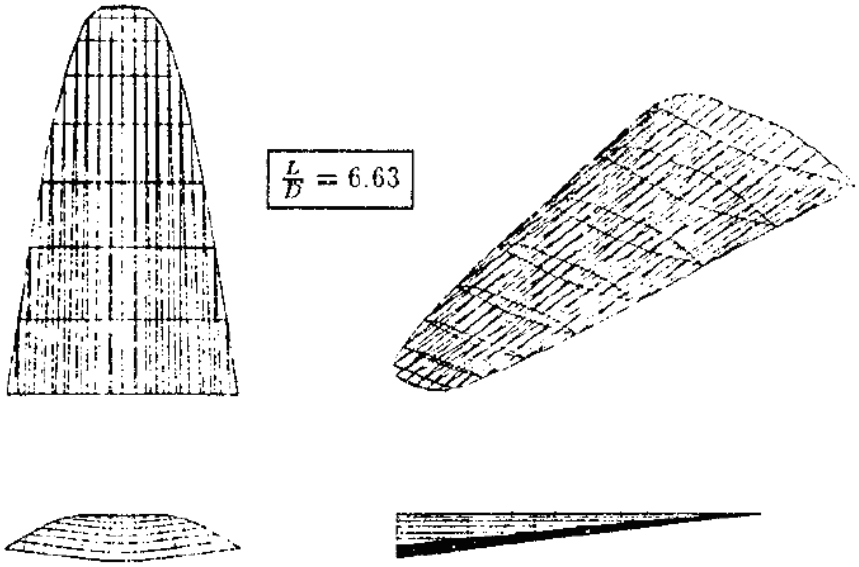

Figure A-6: Waverider Model for Mars & Jupiter [7]

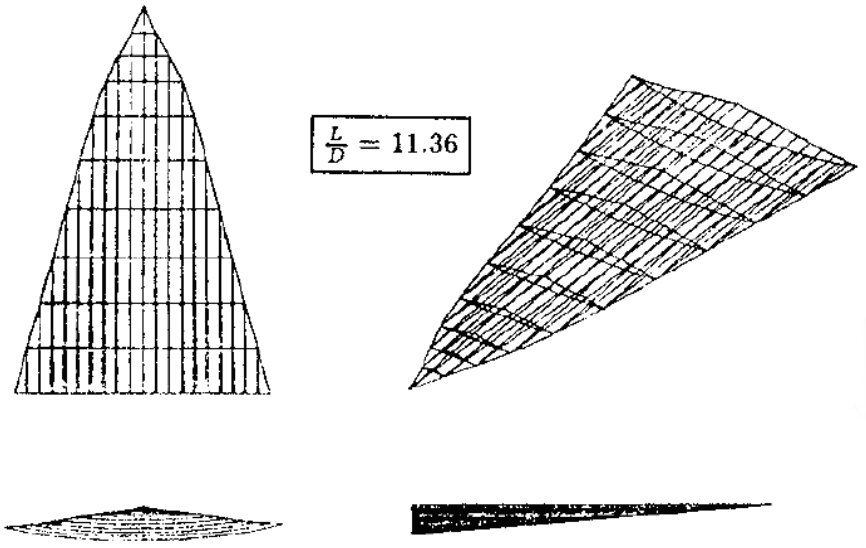

Figure A-7: Waverider Model for Venus 7

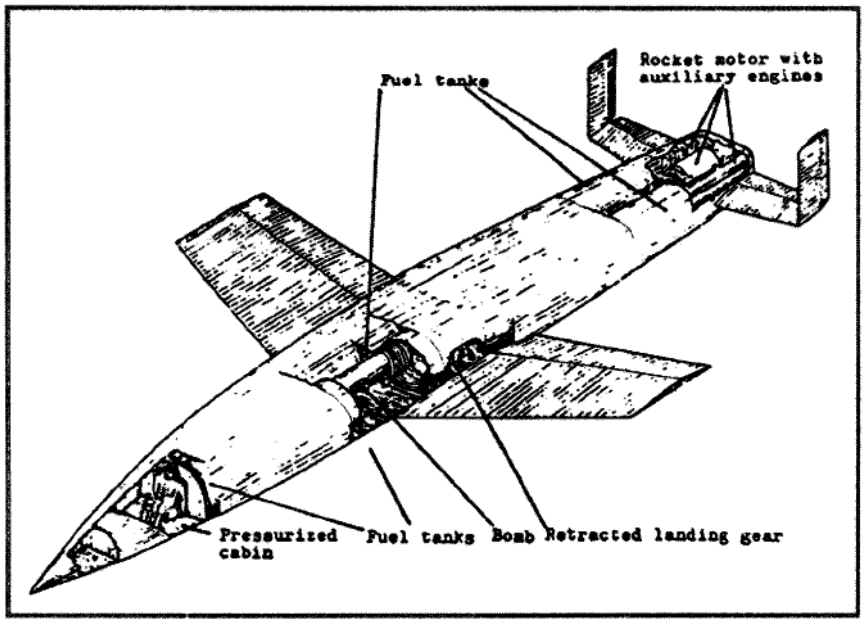

Figure A-8: Sänger-Bredt *Silbervogel* Aircraft[26]

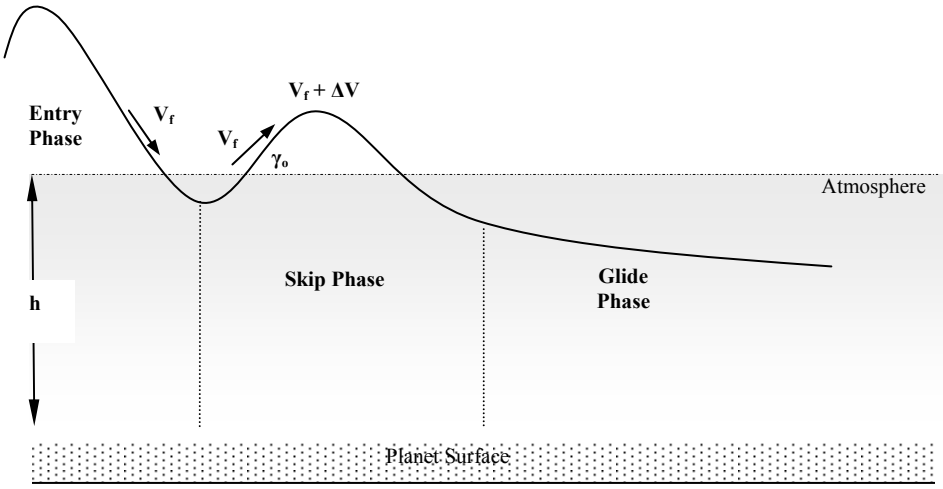

Figure A-9: Parameters of a Periodic Hypersonic Cruise Trajectory

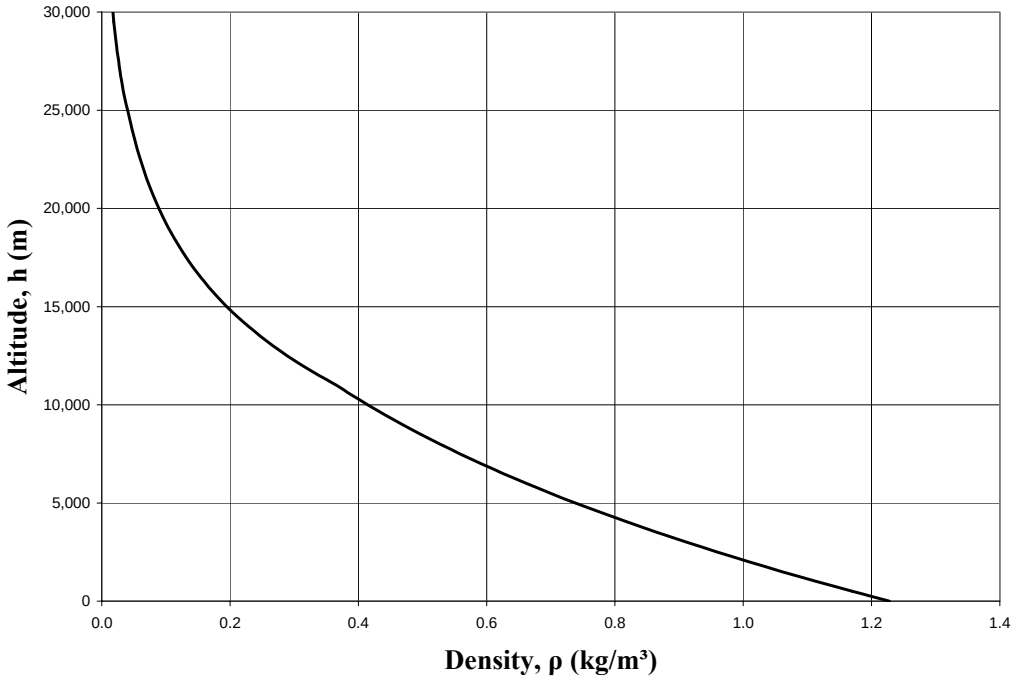

Figure A-10: Altitude vs. Density for Earth

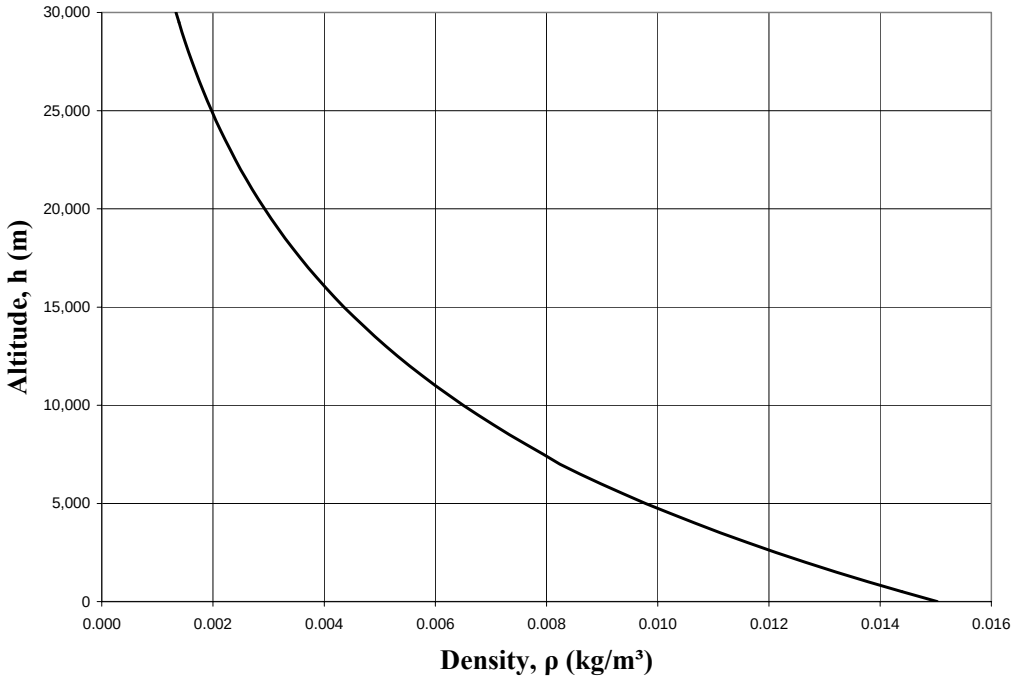

Figure A-11: Altitude vs. Density for Mars

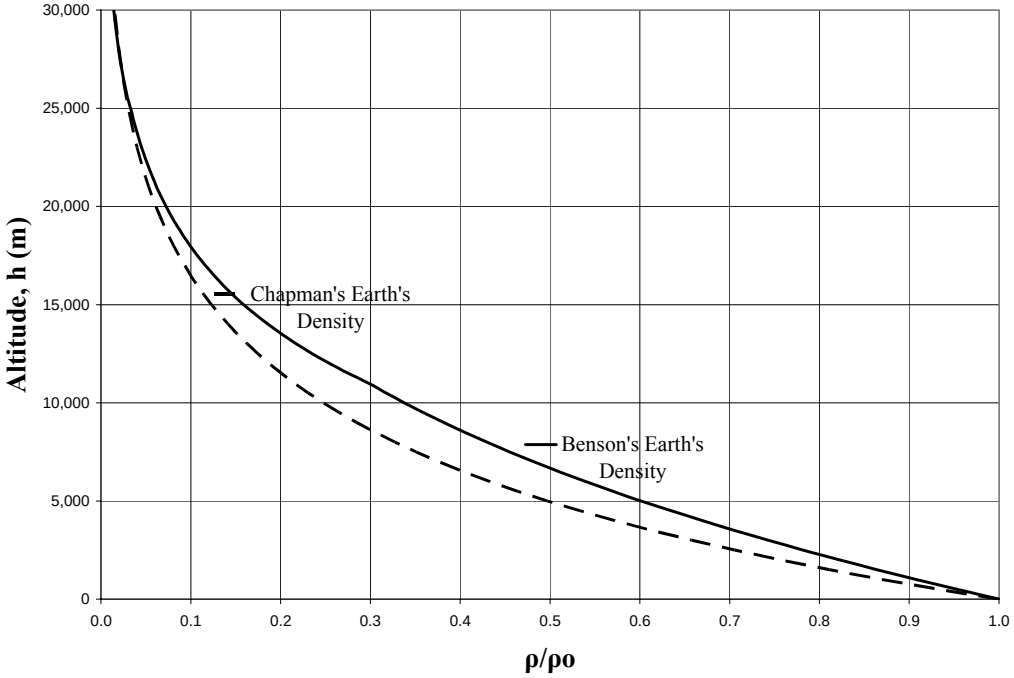

Figure A-12: Altitude vs. ρ/ρo for Earth

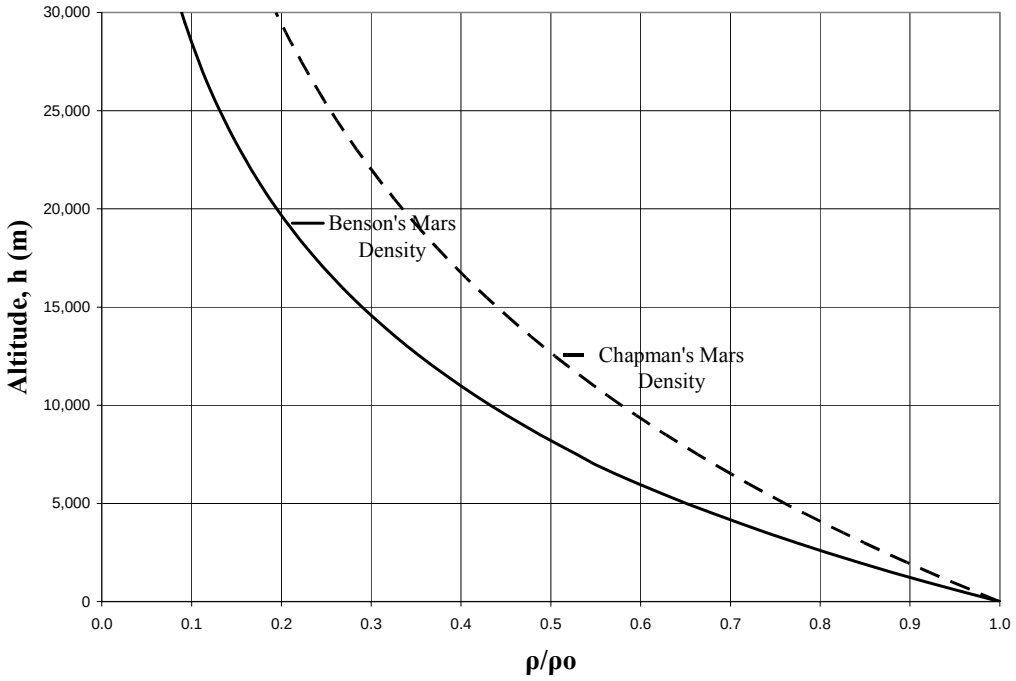

Figure A-13: Altitude vs. ρ/ρo for Mars

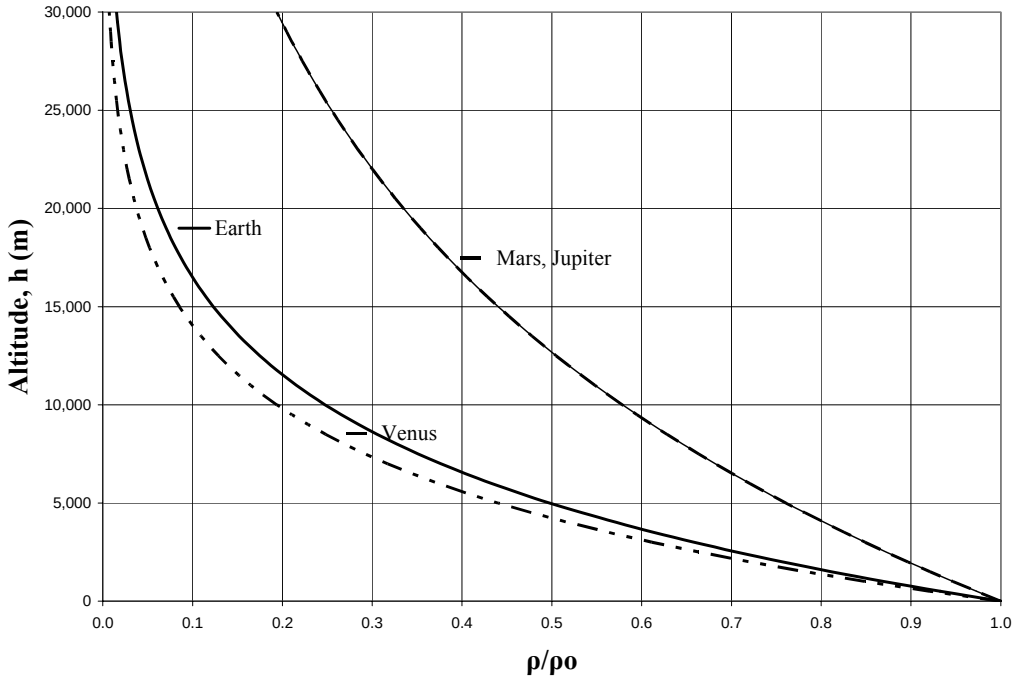

Figure A-14: Altitude vs. ρ/ρo for Various Planets

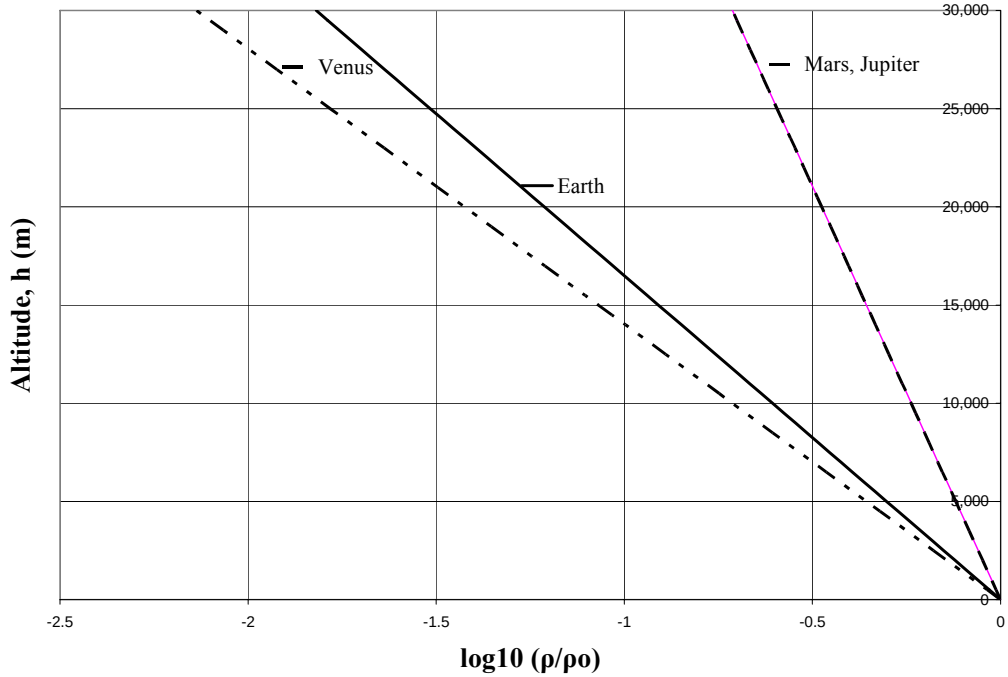

Figure A-15: Altitude vs. $\log_{10}(\rho/\rho_o)$ for Various Planets

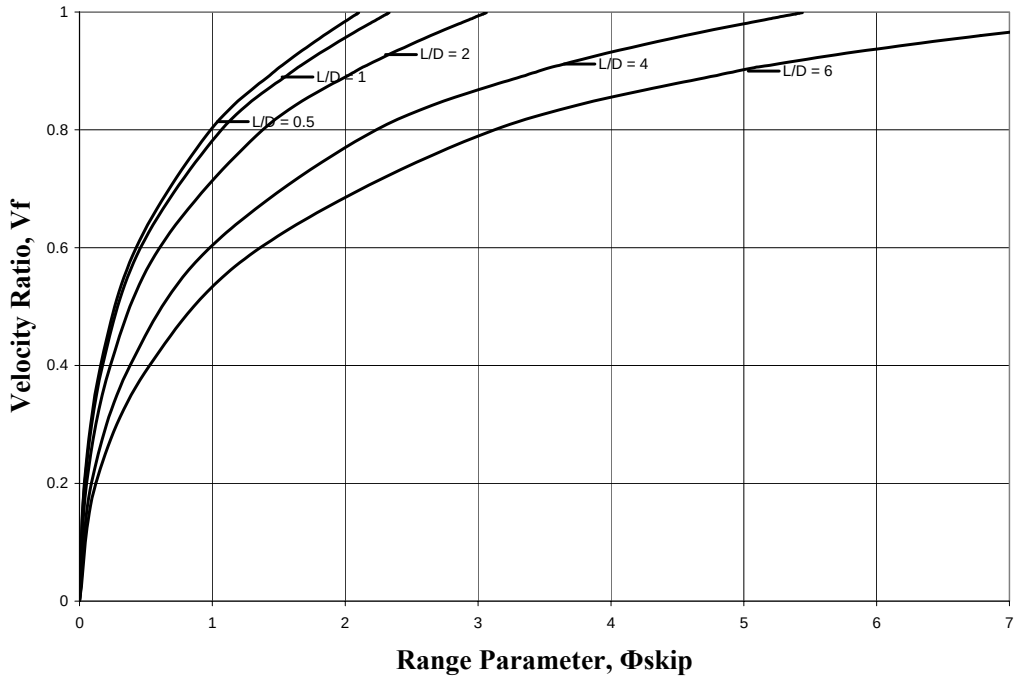

Figure A-16: Velocity Ratio vs. Range Parameter for a Skip Trajectory

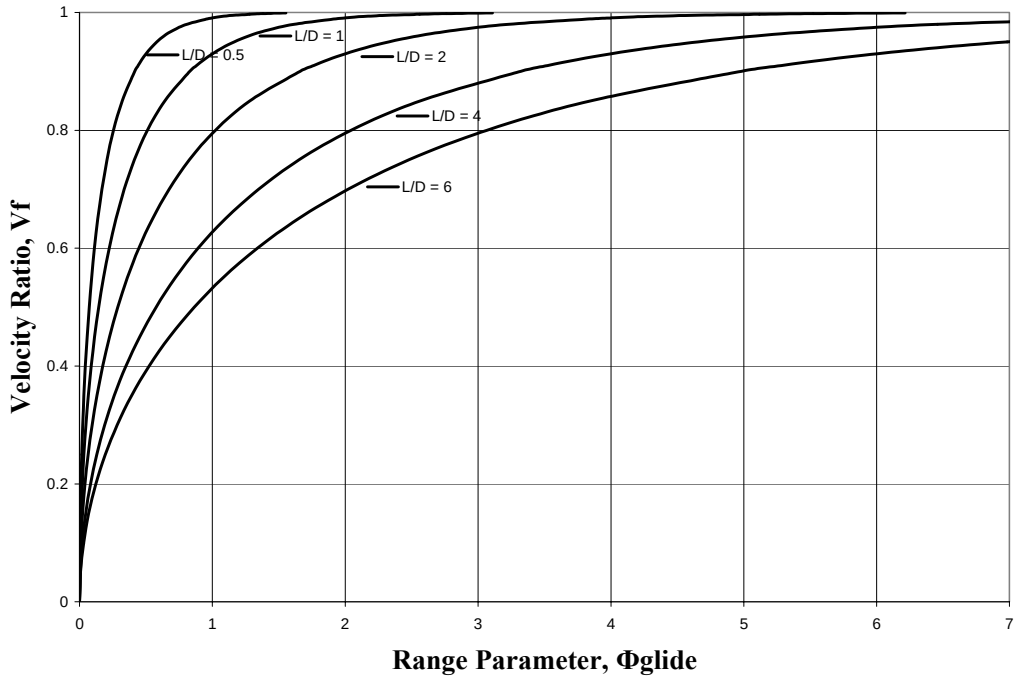

Figure A-17: Velocity Ratio vs. Range Parameter for a Glide Trajectory

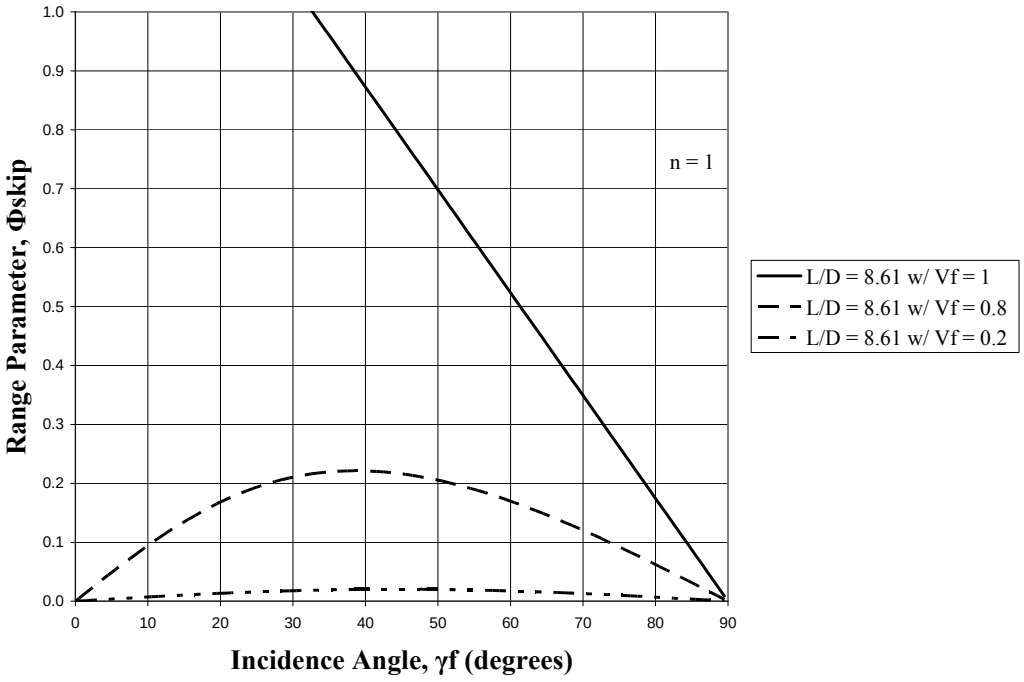

Figure A-18: Range Parameter vs. Incidence Angle for n = 1

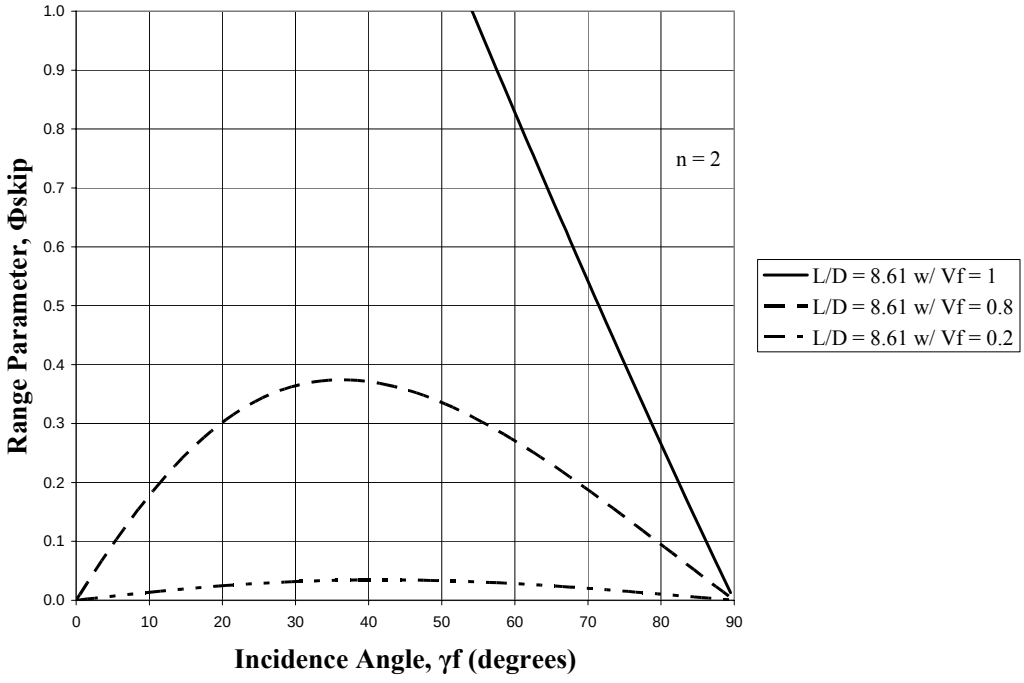

Figure A-19: Range Parameter vs. Incidence Angle for n = 2

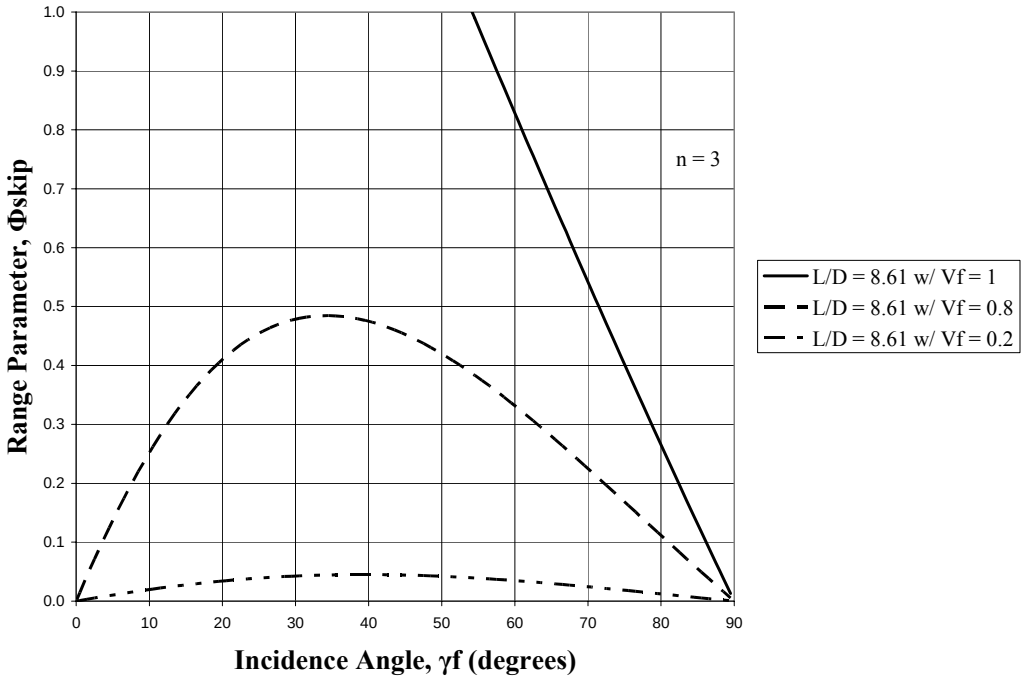

Figure A-20: Range Parameter vs. Incidence Angle for n = 3

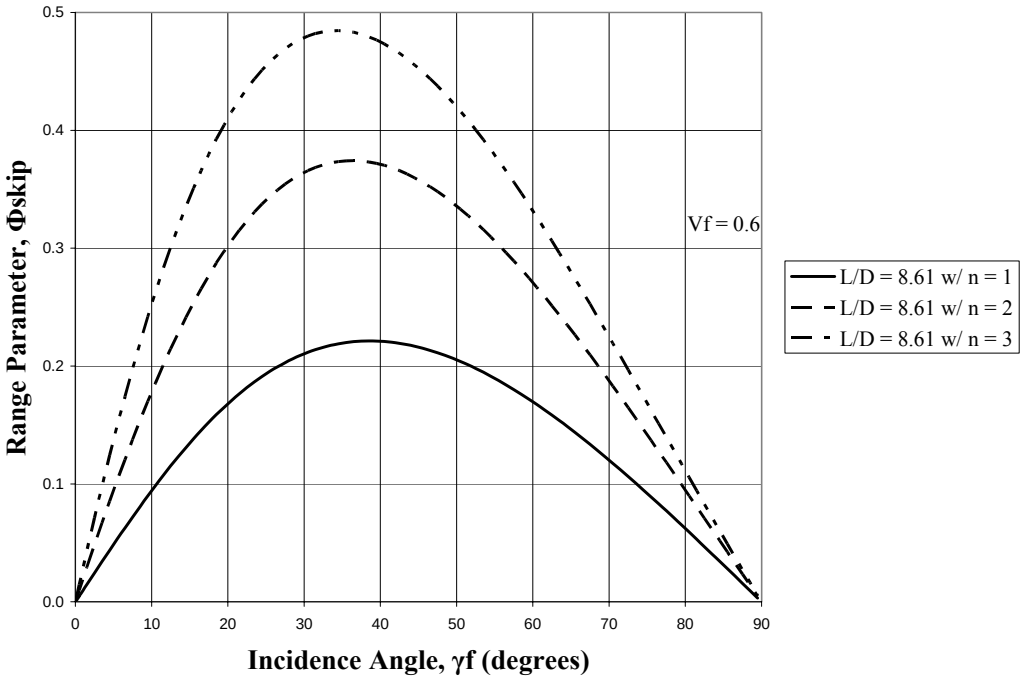

Figure A-21: Range Parameter vs. Incidence Angle for L/D = 8.61 & V_f = 0.6

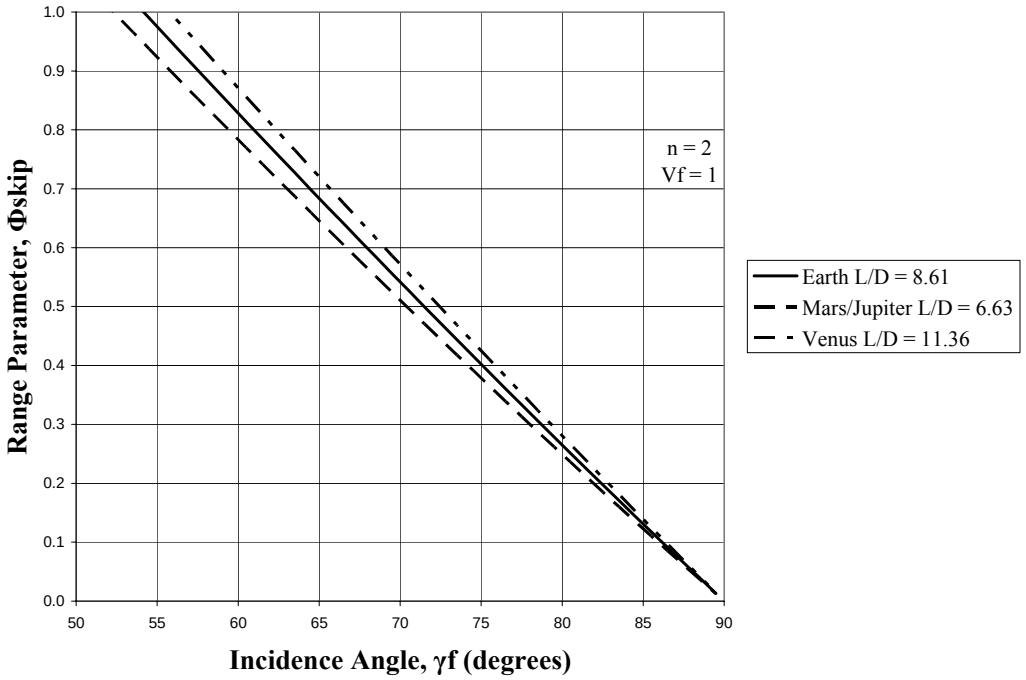

Figure A-22: Various Planets Range Parameter vs. Incidence Angle for n = 2

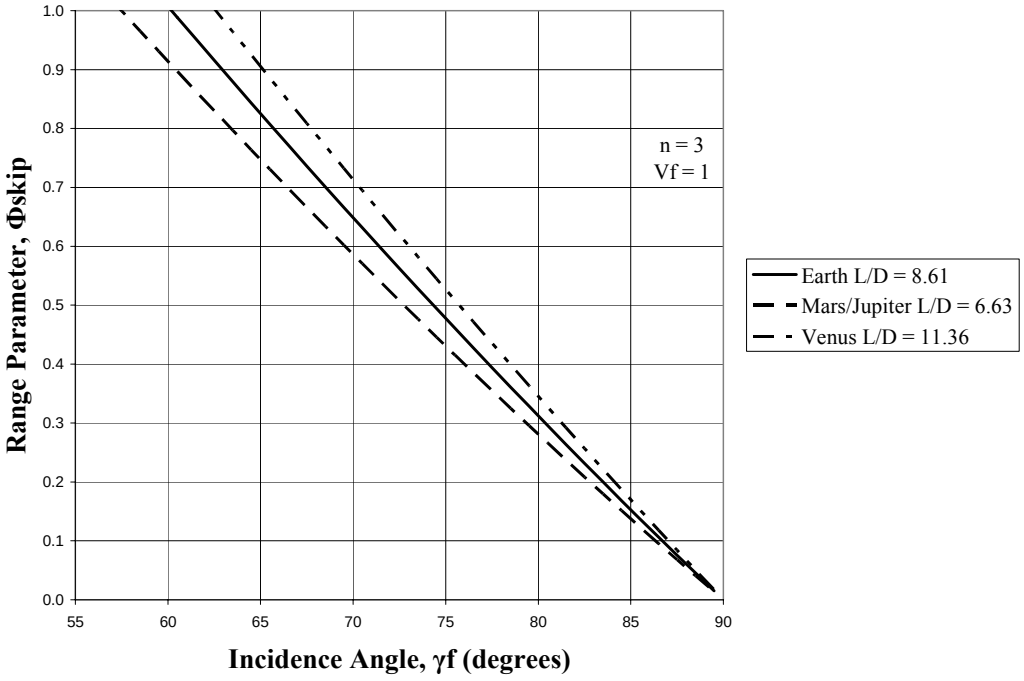

Figure A-23: Various Planets Range Parameter vs. Incidence Angle for n = 3

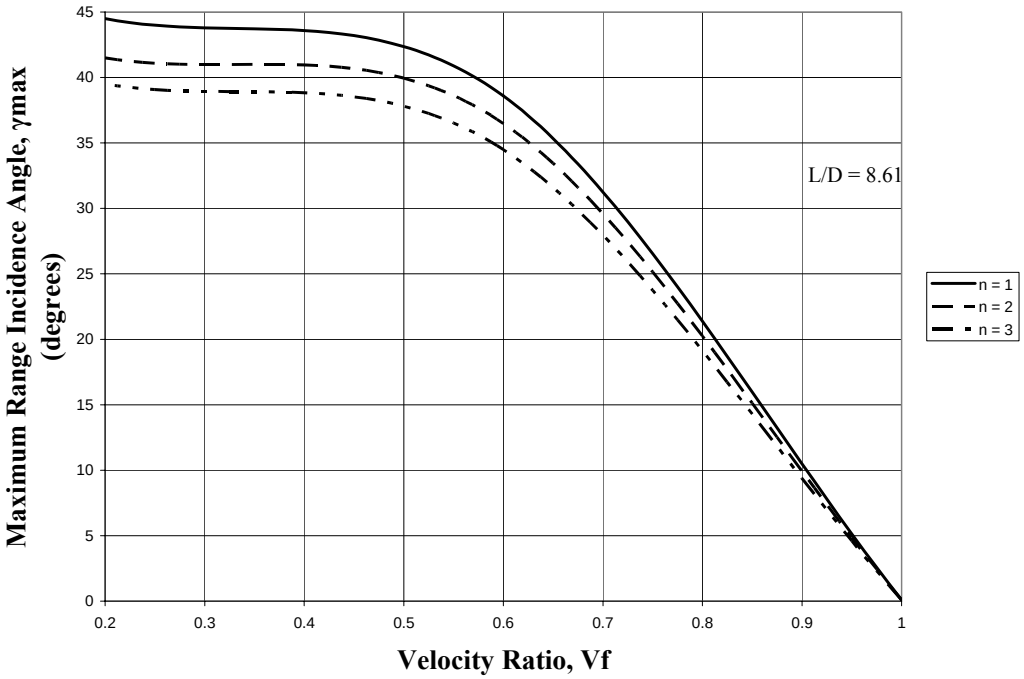

Figure A-24: Max. Range Incidence Angle vs. Velocity Ratio for L/D = 8.61

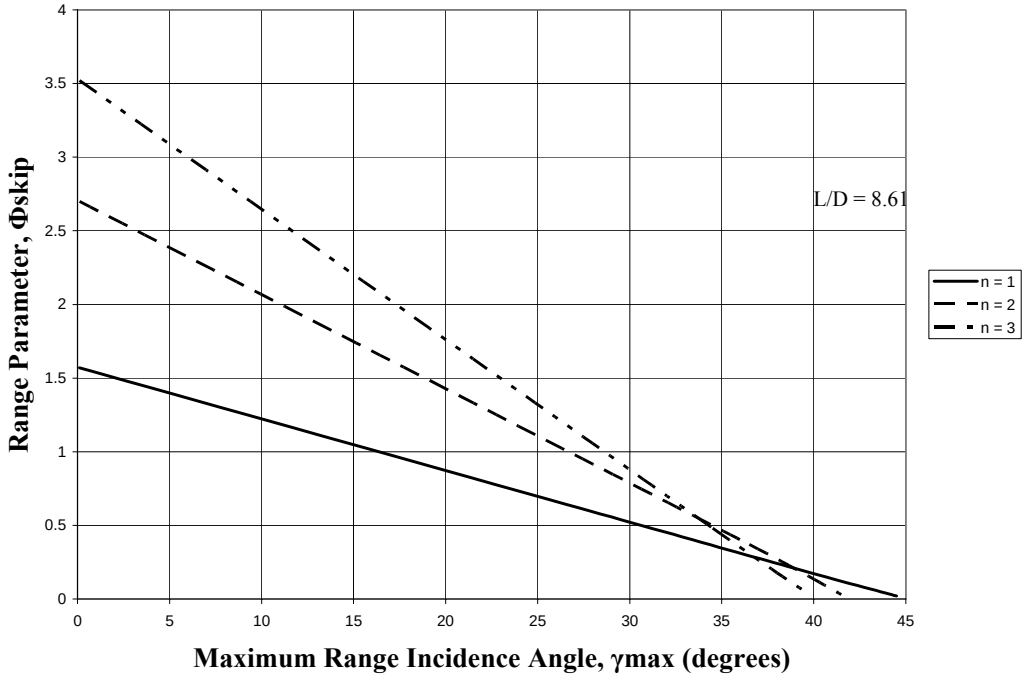

Figure A-25: Range Parameter vs. Max. Range Incidence Angle for L/D = 8.61

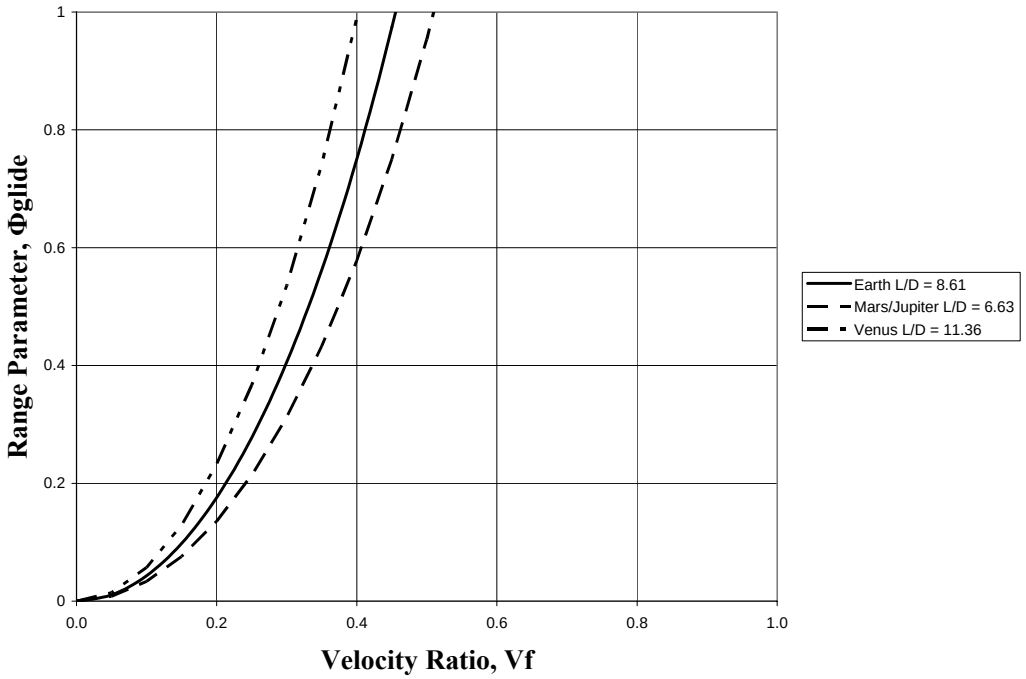

Figure A-26: Range Parameter vs. Velocity Ratio vs. for Various Planets

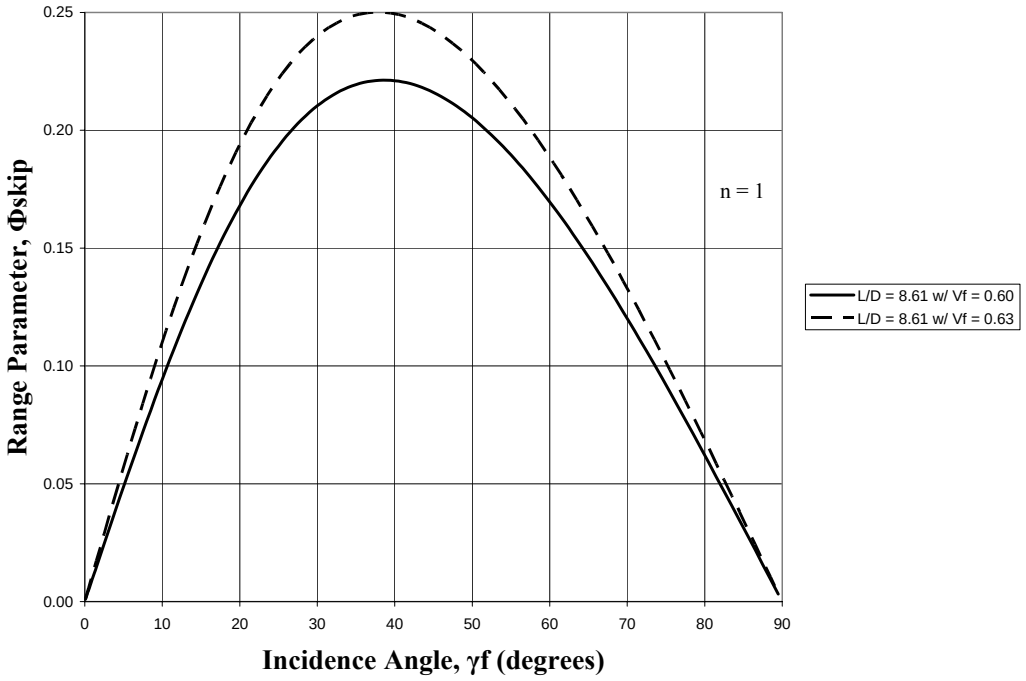

Figure A-27: Earth Range Parameter (Φskip) vs. Incidence Angle (γf) after n = 1

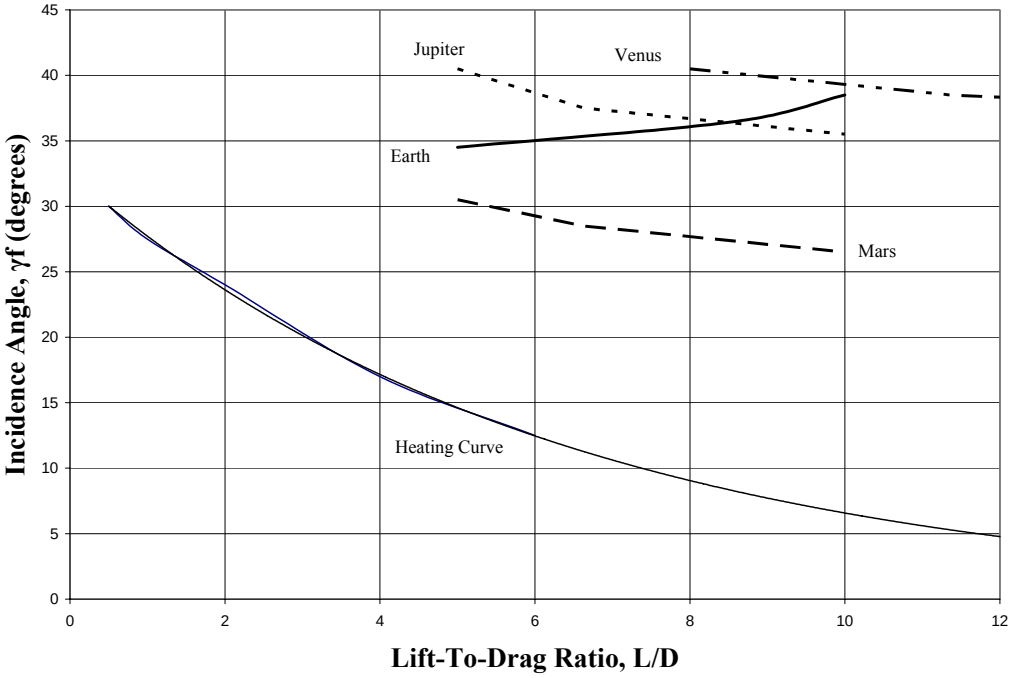

Figure A-28: Incidence Angle vs. Lift-To-Drag Ratio with Heating Curve

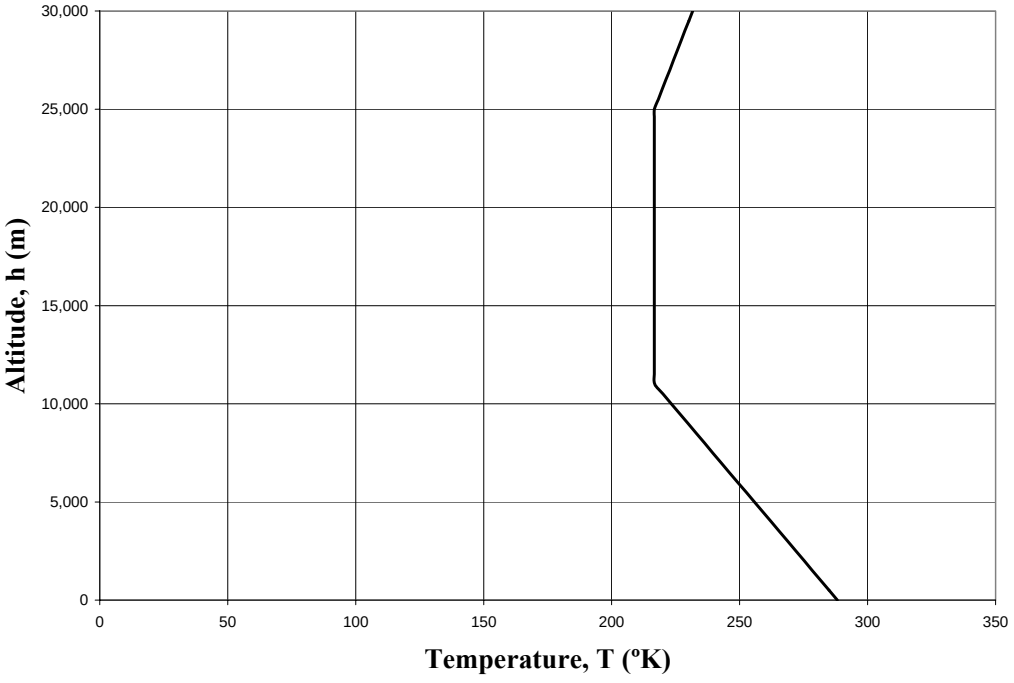

Figure A-29: Altitude vs. Temperature for Earth

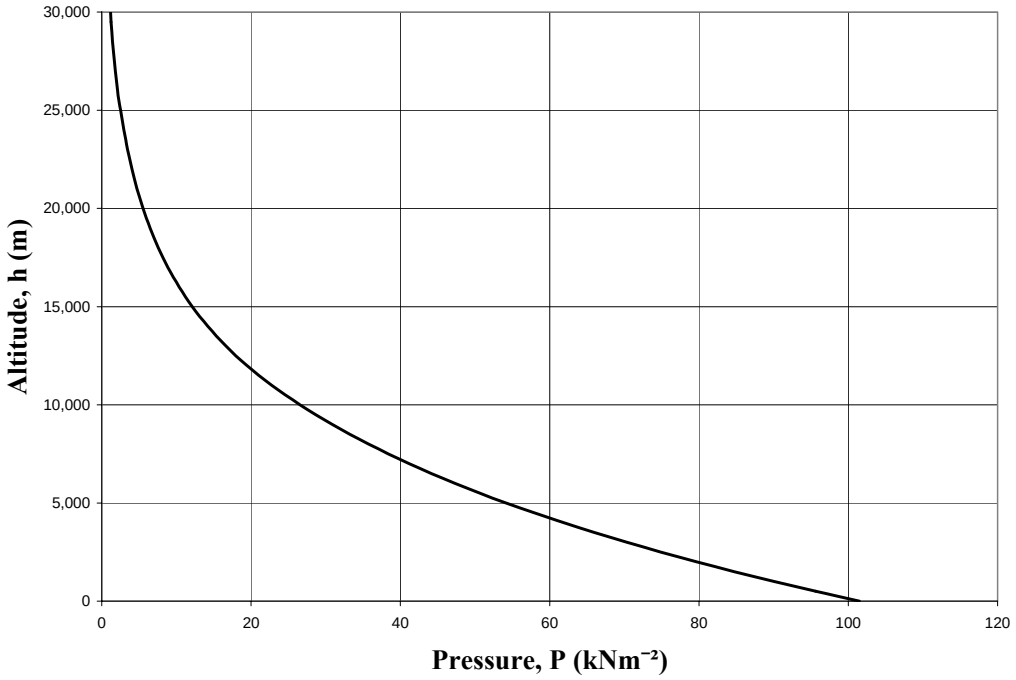

Figure A-30: Altitude vs. Pressure for Earth

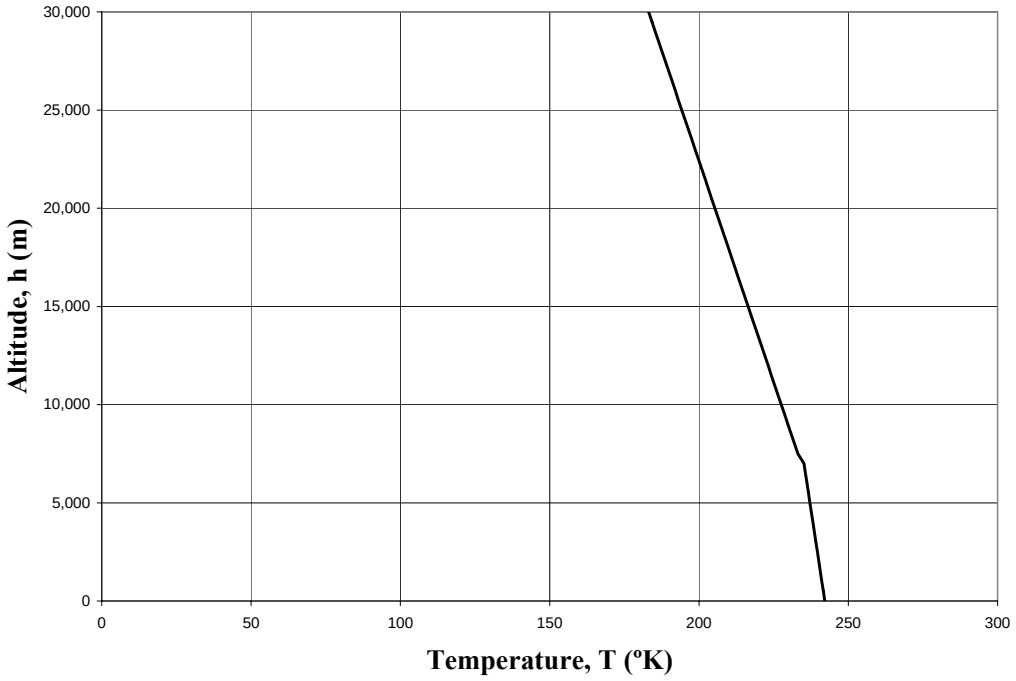

Figure A-31: Altitude vs. Temperature for Mars

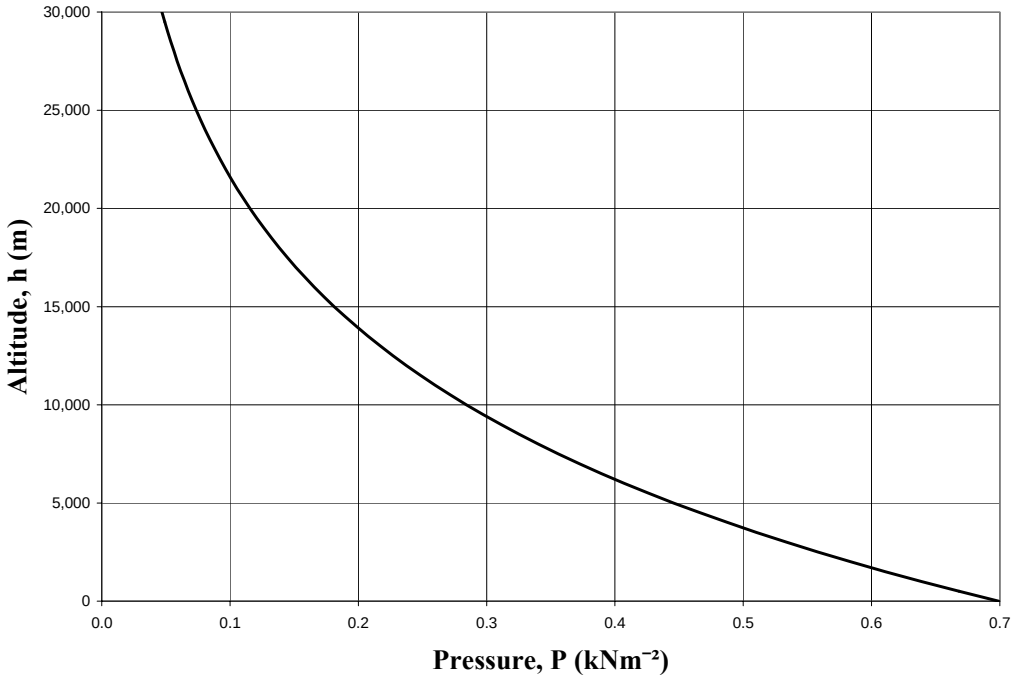

Figure A-32: Altitude vs. Pressure for Mars

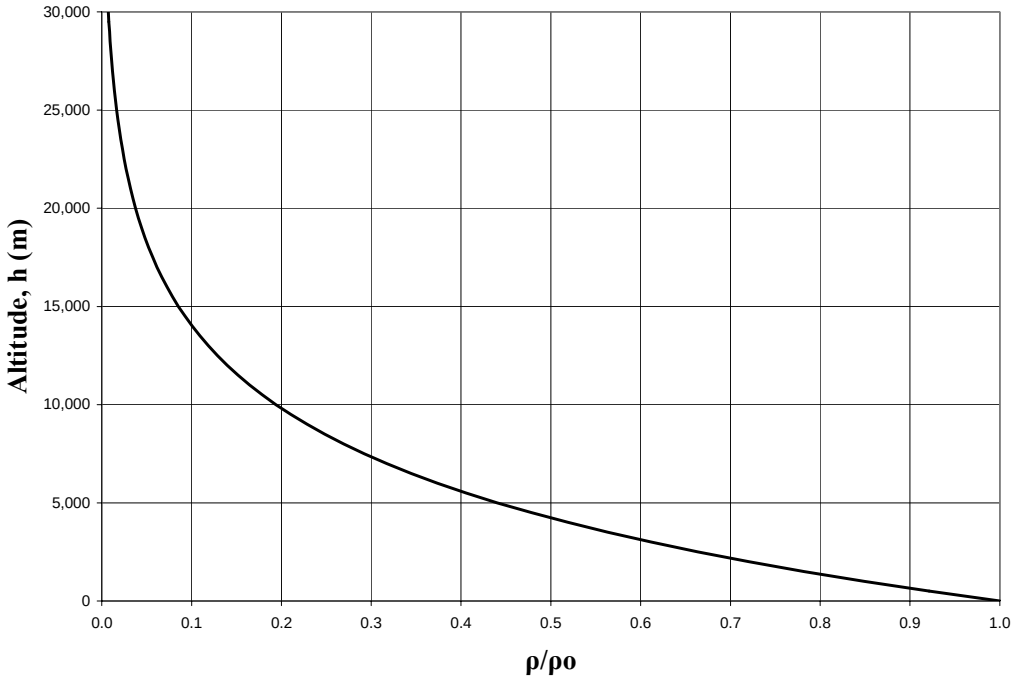

Figure A-33: Altitude vs. ρ/ρ_o for Venus

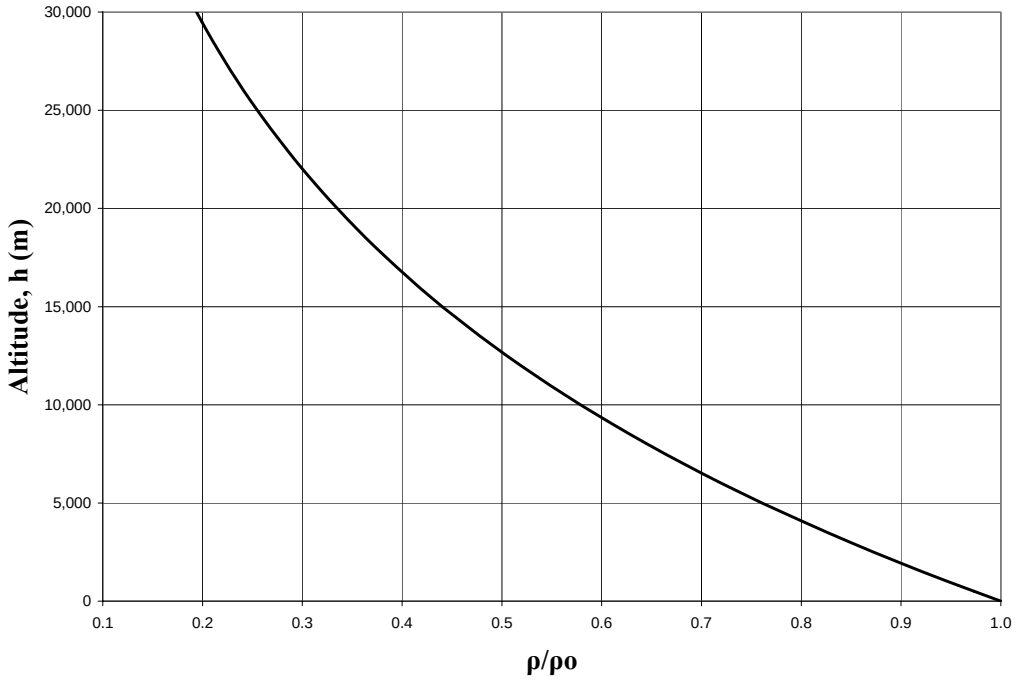

Figure A-34: Altitude vs. ρ/ρ_o for Jupiter

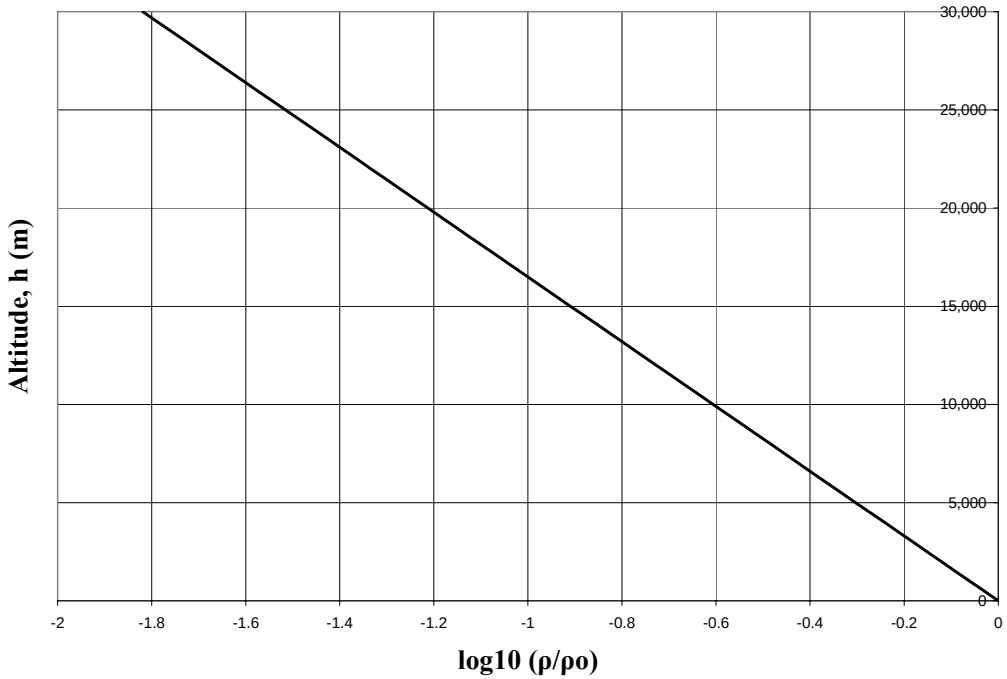

Figure A-35: Altitude vs. $\log_{10}(\rho/\rho_o)$ for Earth

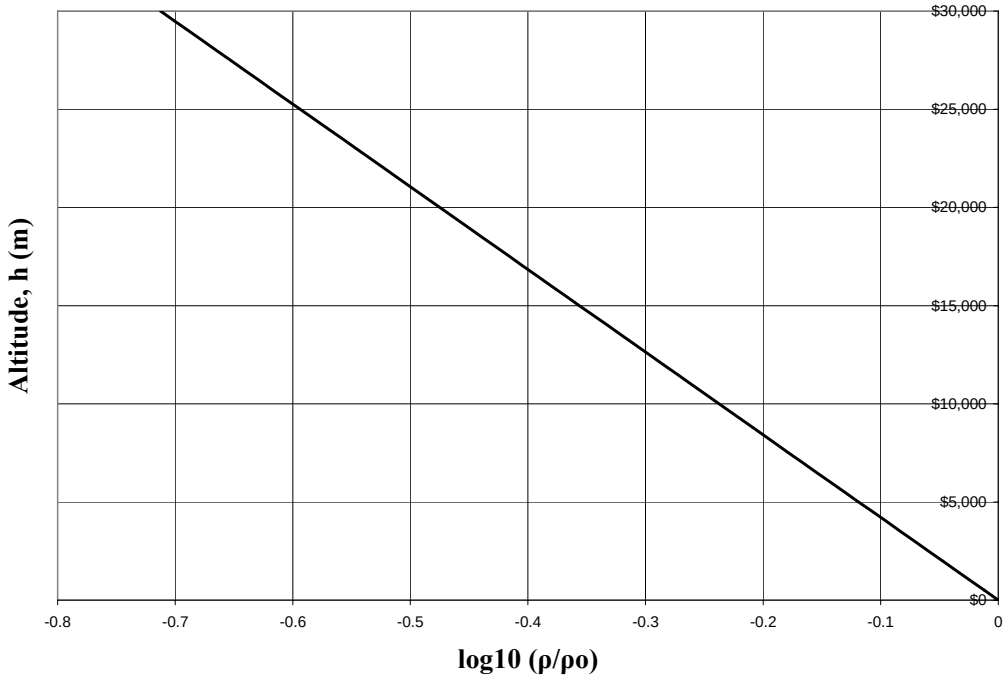

Figure A-36: Altitude vs. $\log_{10}(\rho/\rho_o)$ for Mars

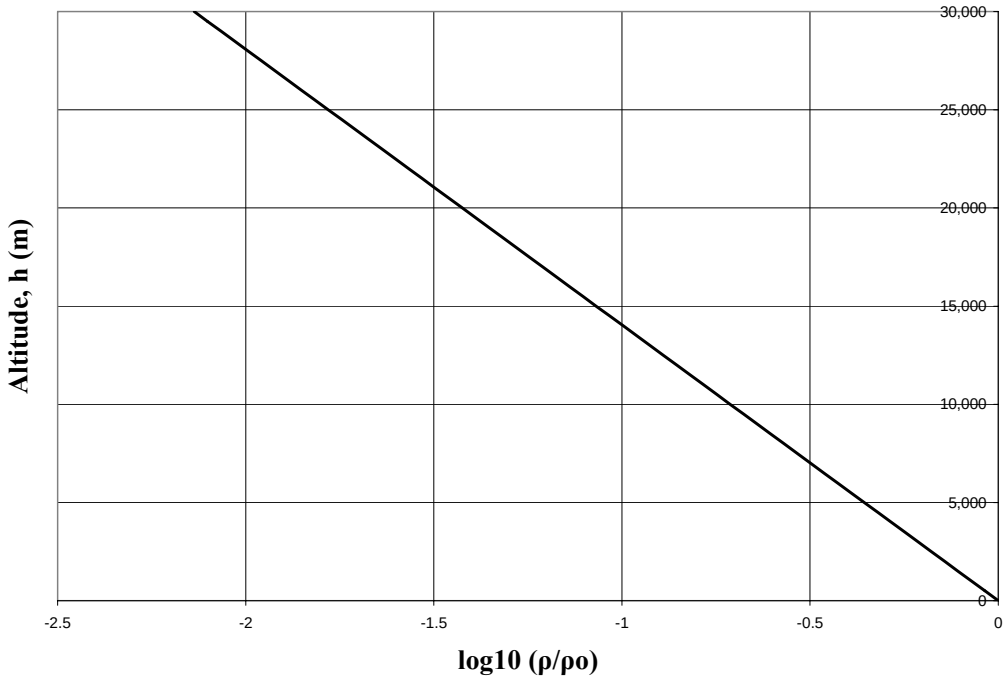

Figure A-37: Altitude vs. $\log_{10}(\rho/\rho_o)$ for Venus

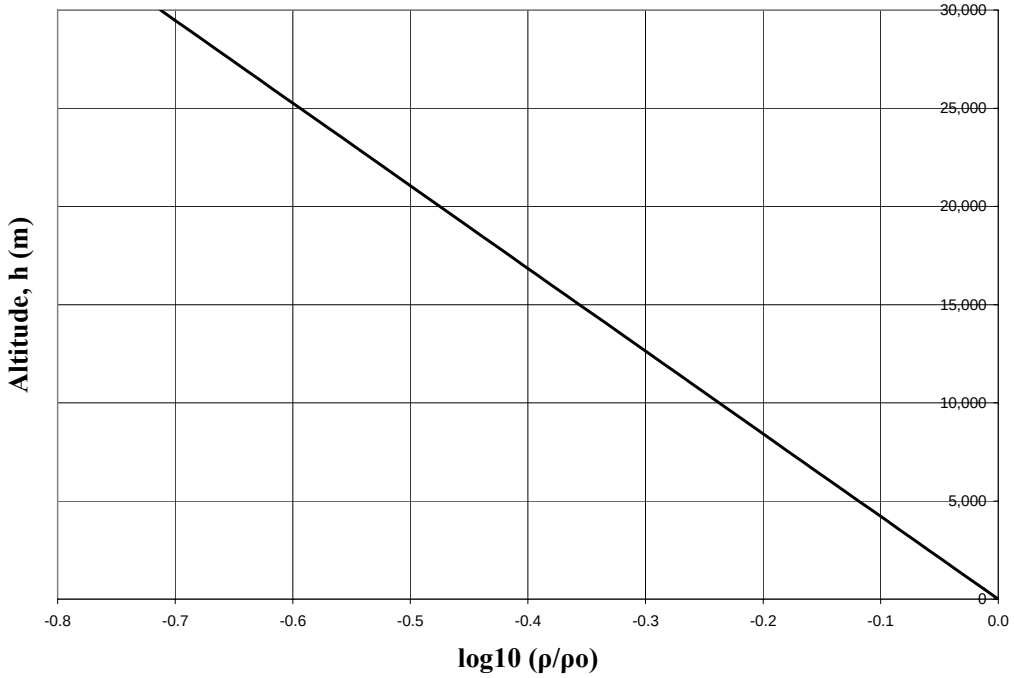

Figure A-38: Altitude vs. $\log_{10}(\rho/\rho_o)$ for Jupiter

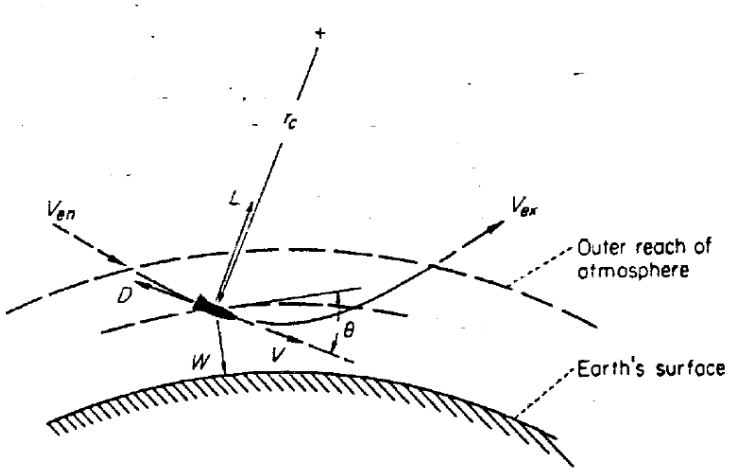

Figure A-39: Sketch of a Vehicle Executing a 'Skip' Trajectory

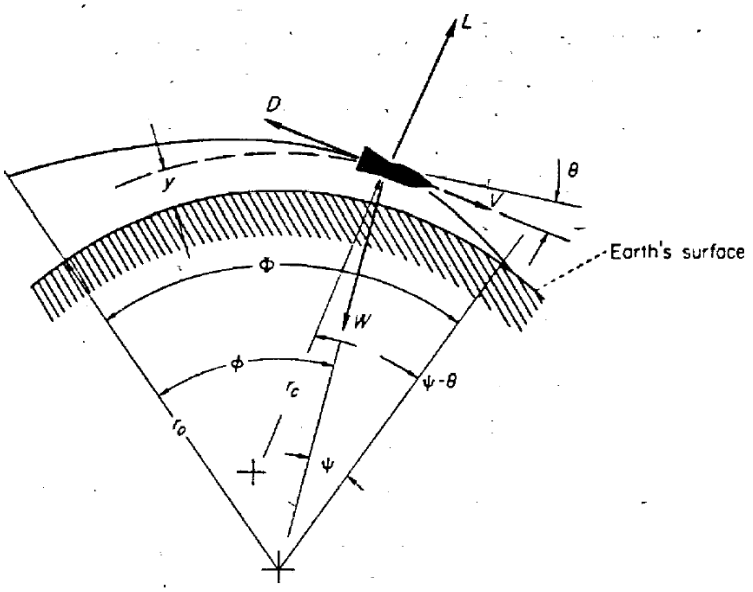

Figure A-40: Sketch of a Vehicle Executing a 'Glide' Trajectory

VITA

Ngoc-Thuy Dang Nguyen was born in Aachen, Germany, on September 28, 1979. She later moved with her family to Hannover before coming to the United States in 1993. As for today, her family currently resides in Virginia. After graduating from J.E.B. Stuart High School in 1998, she studied at Embry Riddle Aeronautical University where she received her Bachelor of Science in Aerospace Engineering with a minor in Mathematics. Ngoc-Thuy is currently pursuing her Master of Science in Aerospace Engineering at the University of Tennessee Space Institute.